Geophys. J. Int. (1991) **104**, 179–201

Palaeomagnetism of red beds of the Late Devonian Worange Point Formation, SE Australia

G. A. Thrupp,[1]* D. V. Kent,[2] P. W. Schmidt[3] and C. McA. Powell[1]†

[1] *Earth Sciences, Macquarie University, NSW* 2109, *Australia*
[2] *Lamont–Doherty Geological Observatory, Palisades, NY* 10964, *USA*
[3] *CSIRO Division of Exploration Geosciences, PO Box* 136, *North Ryde, NSW* 2113, *Australia*

Accepted 1990 August 23. Received 1990 August 22; in original form 1990 April 19

SUMMARY

Gently folded strata of the Late Devonian Merrimbula Group along the south coast of New South Wales are similar to numerous deposits of Late Devonian to Early Carboniferous, subaerial to shallow marine, quartzose sandstone that are known as the Lambie Facies of SE Australia. Because the Lambie sands overlap the early Palaeozoic tectonic elements of the Lachlan Fold Belt, large displacement since the Late Devonian of any Lachlan terranes, with respect to interior Australia, is precluded. We collected oriented core samples from 37 sites primarily in reddish, quartzose litharenites of the Worange Point Formation. The remanent magnetization is carried by haematite. Incremental thermal demagnetization reveals a dominant, well-defined, steep-upward-north component of magnetization that post-dates the mid-Carboniferous folding. The south pole position (146.4°E, 68.6°S, A_{95} 3.1°) derived from the overprinted specimens is close to both the Late Carboniferous and mid-Cretaceous reference poles as well as the spin axis of today. The overprint is attributed to both viscous partial thermoremanent and chemical remanent magnetization (VPTRM and CRM). Its exclusively normal polarity is consistent with a mid-Cretaceous acquisition, perhaps related to the rifting of the SE Australian margin.

A characteristic component of magnetization is isolated between ~660° and ~680 °C in ~30 per cent of the samples. Although a regional fold test of the overall result is inconclusive because the directions of characteristic magnetization are generally close to the axes of folding, two sets of samples from opposite limbs of a local syncline pass a fold test at 90 per cent confidence, indicating a pre-folding origin of the remanence. The presence of both polarities in thin horizons, some of which are palaeosols, and diagenetic haematite associated with incipient cleavage formed in an early stage of deformation before folding, indicates that the acquisition of remanent magnetization occurred over a protracted period. An analysis that combines great circle demagnetization paths and set points, facilitates the incorporation of more data but gives a biassed result. Although normal and reverse polarity subsets are roughly antipodal, residual post-folding components cause the normal subset to fail a fold test. A south pole position (19.7°E, 70.8°S, A_{95} 7.1°) is derived from the specimens with characteristic component of reverse polarity in which the isolation of a characteristic component is clear.

The pole position is close to that of a previous palaeomagnetic study from a widely separated occurrence of Lambie Facies sediments; both results are applicable not only to the Lachlan Fold belt, but also to the rest of Australia, and Gondwana as a whole. The position of the two poles derived from the Lambie Facies overlap assemblage in the Lachlan Fold Belt supports the interpretation that the progression

* Present address: Mackie Martin and Associates, 16 Hunter Street, Hornsby, NSW 2077, Australia.
† Present address: Department of Geology, University Western Australia, Nedlands, WA 6009, Australia.

of Australian poles derived from mid to Late Devonian rocks reflects Gondwanan drift from mid-Devonian to mid-Carboniferous, and does not require rotation of SE Australia relative to the Australian craton since the mid-Devonian.

Key words: demagnetization planes, Devonian, Gondwana, palaeomagnetism, red beds, Tasman Orogen.

INTRODUCTION AND BACKGROUND

Apparent discordance between palaeomagnetic results from early Palaeozoic rocks in SE Australia and results from rocks of similar age in central and northern Australia, was interpreted as evidence for azimuthal rotation, prior to the Late Devonian, of tectonic elements of the Tasman orogen relative to the rest of Australia (McElhinny & Embleton 1974; Embleton *et al.* 1974). Belts of serpentinite and ultramafic rocks within the Tasman orogen of eastern Australia were suggested to represent possible Palaeozoic suture zones (e.g. Embleton *et al.* 1974). Tectonostratigraphic analyses resulted in the delineation of numerous terranes in the Tasman Orogen (Scheibner 1985; Leitch & Scheibner 1987, and companion papers).

A constraint on the timing of consolidation of the SE Tasman terranes is provided by the Late Devonian–Early Carboniferous Lambie Facies. The term 'Lambie Stage' was coined by Brown (1931) for Late Devonian shallow marine quartzose sediments that had been named after the exposure at Mt Lambie (Benson 1922). Brown (1931) suggested that although the Lambie sediments are best preserved in restricted, 'narrow synclinal troughs', they originally were a widespread 'veneer of arenaceous sediments.' Also, the regional structural and stratigraphic relationships were interpreted (e.g. Conolly 1969; McIlveen 1975) to suggest that the Lambie Group sediments were initially part of a nearly continuous sheet that was deposited after mid-Devonian folding associated with the Tabberabberan Orogeny (e.g. VandenBerg 1976). Palaeocurrent studies show that the Lambie Facies were derived principally from the craton and prograded eastward across the Tasman Orogen (e.g. Powell 1984; Powell *et al.* 1990). The Lambie Facies is thus an overlap assemblage (see Fig. 1) that precludes major displacement of the SE Tasman terranes after the mid-Devonian folding.

The common provenance and facies of Silurian and Devonian rocks in SE Australia was noted by McElhinny & Embleton (1974) as evidence against gross displacement of Tasman terranes to explain the disparate Tasman Siluro-Devonian palaeomagnetic poles. Instead, to explain the palaeomagnetic data they (Embleton *et al.* 1974; McElhinny & Embleton 1974) suggested a 90°, essentially *in situ,* counterclockwise azimuthal rotation during Middle Silurian to Early Carboniferous time (30° since Early Devonian) of a SE Tasman terrane with respect to the craton. Alternatively, APWPs (apparent polar wander paths: relative positions through time of tectonic plates to the spin axis of the Earth) were proposed that incorporated the SE Australian poles and thus obviated the need for rotation or an exotic Tasman terrane: one alternative APWP accommodated the SE Australian poles by adopting the opposite polarity for the early Palaeozoic palaeomagnetic poles from central and northern Australia (Schmidt & Morris 1977). Two others had a large Siluro-Devonian loop (Morel & Irving 1978; Goleby 1980). Fig. 2 depicts the four versions of the evolving Australian APWP.

The rotated Tasman terrane model (Embleton *et al.* 1974; McElhinny & Embleton 1974) was based primarily on the comparison of two palaeomagnetic poles. One is from the Mereenie Sandstone of central Australia (MS; Embleton 1972), the other is from a compilation of results from Silurian volcanic rocks of SE Australia (SV; Luck 1973). Scrutiny of these studies, however, reveals that the two pole positions may be highly unreliable. Neither has a 'fold test' to constrain the relative timing of tectonic tilting and acquisition of magnetization. The control on palaeohorizontal of the Silurian volcanics is, at best, poor. The Mereenie Sandstone (MS) data are very scattered even after many samples are omitted. Before correction for tilt, the MS pole position is close to poles that are believed to be mid-Carboniferous. If the magnetization of tilted strata is not original, and there is no 'fold test', then the attitude at the time of overprinting is unknown. Thus, the rotated Tasman terrane model was founded on two palaeomagnetic poles of dubious reliability. A new palaeomagnetic study of the MS suggests that the original result was plagued by incompletely removed secondary overprints; the revised MS pole position is completely different (Li *et al.* 1990a). The new result, however, also lacks a fold test.

Several new Australian Palaeozoic palaeomagnetic poles of relatively high quality are utilized in the construction of amended APWPs for Gondwana (Schmidt *et al.* 1986; Schmidt, Embleton & Palmer 1987; Schmidt & Embleton 1987; Li, Schmidt & Embleton 1988; Li *et al.* 1990b; Schmidt *et al.* 1990). The majority of the poles are the results of palaeomagnetic studies of Palaeozoic rocks of the Lachlan Fold Belt, a tectonic province in the SE part of the Tasman Orogen (Figs 1 and 3). Two high-quality Devonian palaeomagnetic results from lavas of the Lachlan Fold Belt were claimed to apply to Australia and Gondwana (CV: Comerong Volcanics and SRV: Snowy River Volcanics; Schmidt *et al.* 1986, 1987). However, an azimuthal difference of 37.5° between poles derived from Frasnian to Famennian (Late Devonian) limestones of the Canning Basin (CB) and the Givetian to Frasnian (mid-Devonian) lavas of the Comerong Volcanics (CV) from the Lachlan Fold Belt was interpreted again as evidence for rotation or post-mid-Devonian docking of allochthonous elements of the Tasman Orogen (Hurley & Van der Voo 1987). An alternative explanation is that the magnetization of the CB limestones was acquired substantially later than deposition; if so, the difference between the CV and CB pole positions can be attributed to reasonable rates of plate motion during the Late Devonian (Schmidt *et al.* 1987).

The similarity in position of the Canning Basin palaeomagnetic pole and a pole (Li *et al.* 1988) derived from

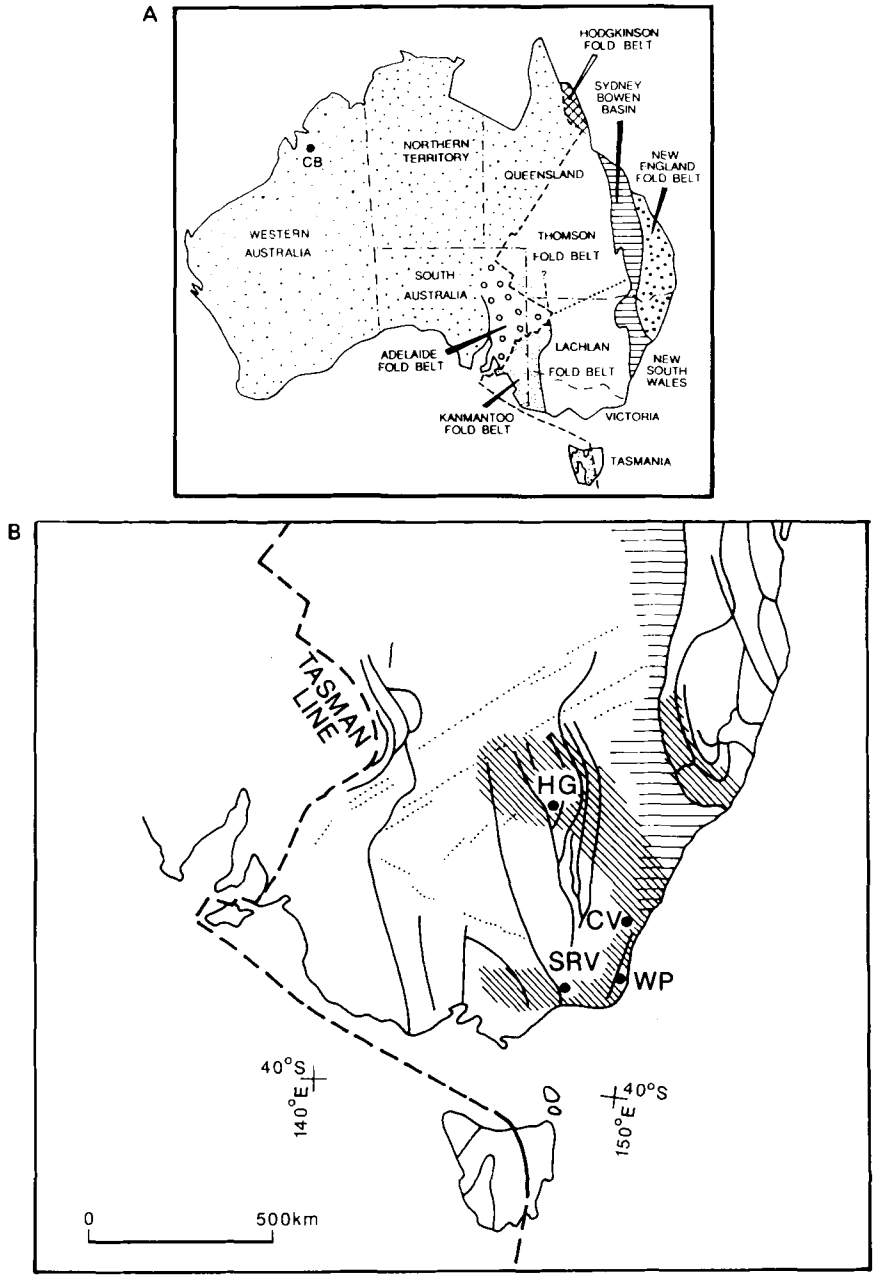

Figure 1. (A) Map of Australia showing major tectonic provinces in the east. (B) Enlargement of SE Australia showing the principal tectonic elements of the southern Tasman Orogen (after Leitch & Scheibner 1987). Major lithotectonic terranes are deliniated. Finely ruled regions represent the original extent of the Late Devonian–Early Carboniferous Lambie Facies overlap assemblage as envisaged by Brown (1931). Coarse horizontal ruling shows the extent of the Permo-Triassic Sydney–Bowen Basin. Tasman Line marks the eastern extent of exposures of Precambrian crust. Mnemonics identify locations of palaeomagnetic studies that are discussed in this paper. SRV: Snowy River Volcanics (Schmidt *et al.* 1987); WP: Worange Point Formation (this study); CV: Commerong Volcanics (Schmidt *et al.* 1986); HG: Hervey Group (Li *et al.* 1988); CB: Canning Basin limestones (Hurley & Van der Voo 1987) on inset showing all of Australia.

red beds of the Hervey Group (HG), a Famennian/Early Carboniferous Lambie Facies locality in the NE Lachlan Fold Belt, supports the interpretation that the Lambie Facies overlap assemblage constrains the timing of displacement of Tasman terranes in the Lachlan Fold Belt. Although the palaeomagnetic and geologic evidence seems to preclude appreciable rotation or displacement of the SE Tasman terranes, at least since the Frasnian time, the Palaeozoic palaeomagnetic poles from the Lachlan Fold Belt are not included in a compilation of poles to constrain the APWP of Gondwana (Van der Voo 1988). Curiously, although, Van der Voo does not consider the early Devonian SRV pole (Schmidt *et al.* 1987) to be applicable to Gondwana, he claims that the close proximity of the SRV pole to an interpolated Early Devonian Gondwanan pole supports the validity of the interpolated pole position.

To investigate the tectonic coherence of the Lachlan Fold Belt, the Lambie Facies overlap constraint, the global position of Australia and Gondwana, and the magnetization of red beds, we collected samples of the Late Devonian

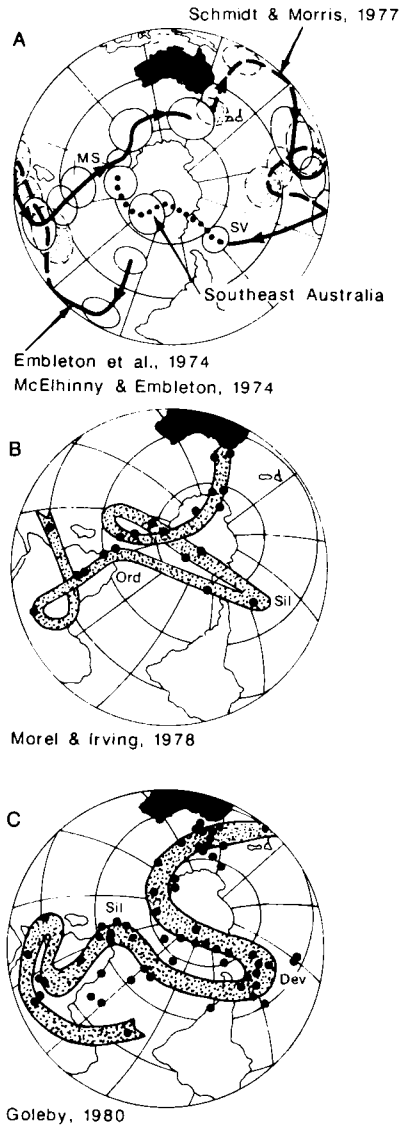

Figure 2. Evolution of the Australian Palaeozoic APWP during the 1970s. (A) Stippled ovals are A_{95}s about south poles in the northern hemisphere. Embleton *et al.* (1974) APWP path with 'discordant' Tasman poles (dotted APWP segment) was believed to be evidence for an exotic SE Australia. MS and SV, the two poles on which the discordant Tasman model hinges, are now recognized to be of unacceptable quality. Alternative APWP suggested by Schmidt & Morris (1977) adopts the opposite polarity for the early Palaeozoic poles, and the Tasman poles are concordant. (B) Morel & Irving (1978) APWP retains Embleton *et al.* (1974) polarity choices, but incorporates the Tasman poles by introducing a large loop in the path. (C) Goleby (1980) path uses the same polarity choices, and incorporates the Tasman poles with a large Siluro-Devonian loop. Note that the apex of the large loop is Silurian in (B) and Devonian in (C).

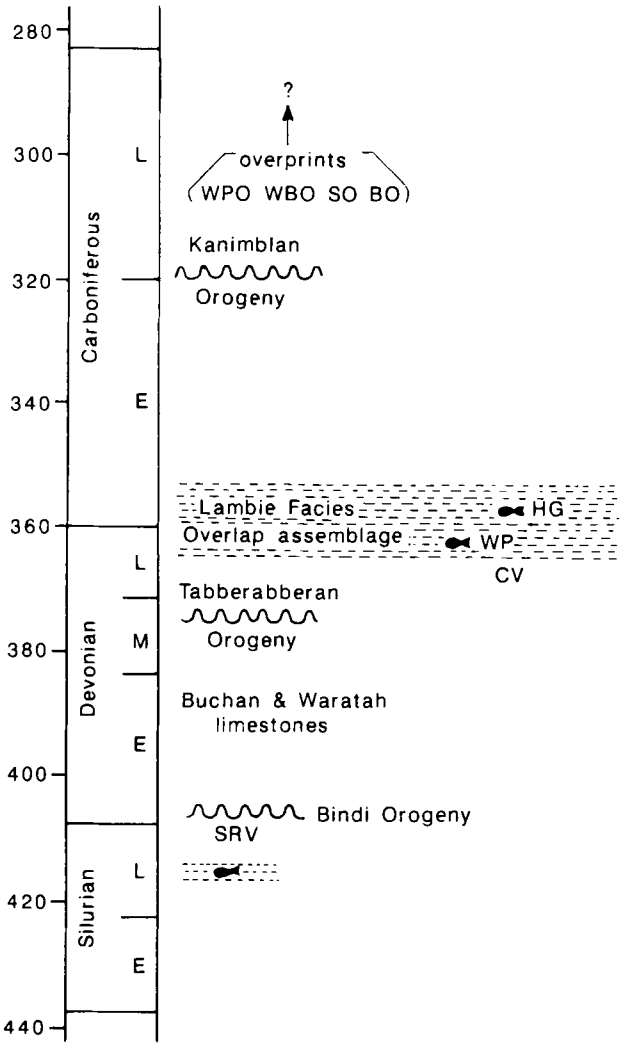

Figure 3. Schematic representation of major periods deformation and temporal relationships of the new palaeomagnetic poles in Palaeozoic rocks of the Lachlan Fold Belt. Fish represent fossil age control; dashed ruling represents sedimentary rocks. Mnemonics represent palaeomagnetic studies as listed in the caption to Fig. 1, and the following overprint palaeomagnetic results. WPO: Worange Point Formation overprint (this study); WBO: Waratah Bay limestone overprint (G. A. Thrupp, unpublished data); SO: Snowy River Volcanics overprint (Schmidt *et al.* 1987); BO: Buchan limestones overprint (Schmidt *et al.* 1987).

Worange Point Formation from the south coast of New South Wales for palaeomagnetic analysis.

GEOLOGY

Gently folded strata of the Late Devonian to Early Carboniferous Merrimbula Group are well exposed along the coast and in road cuts in SE New South Wales (Fig. 4).

We collected oriented core samples from 37 sites (each site a sedimentary horizon) primarily in the Worange Point Formation, the uppermost Merrimbula Group unit (Fig. 5). The sandstones and mudstones of the Worange Point Formation are moderately to well sorted, subangular to subrounded, quartzose litharenites. Most are reddish in colour. Numerous fining-upward fluvial sequences, as well as fine-grained overbank deposits associated with non-cyclic sandstone units, represent typical Lambie Facies deposits of a wide meandering river belt on a coastal plain. The palaeoslope was generally eastward, and the principal source of the Worange Point Formation detritus was the underlying Ordovician quartzose flysch (Steiner 1975; Powell 1983; Taylor & Mayer 1990).

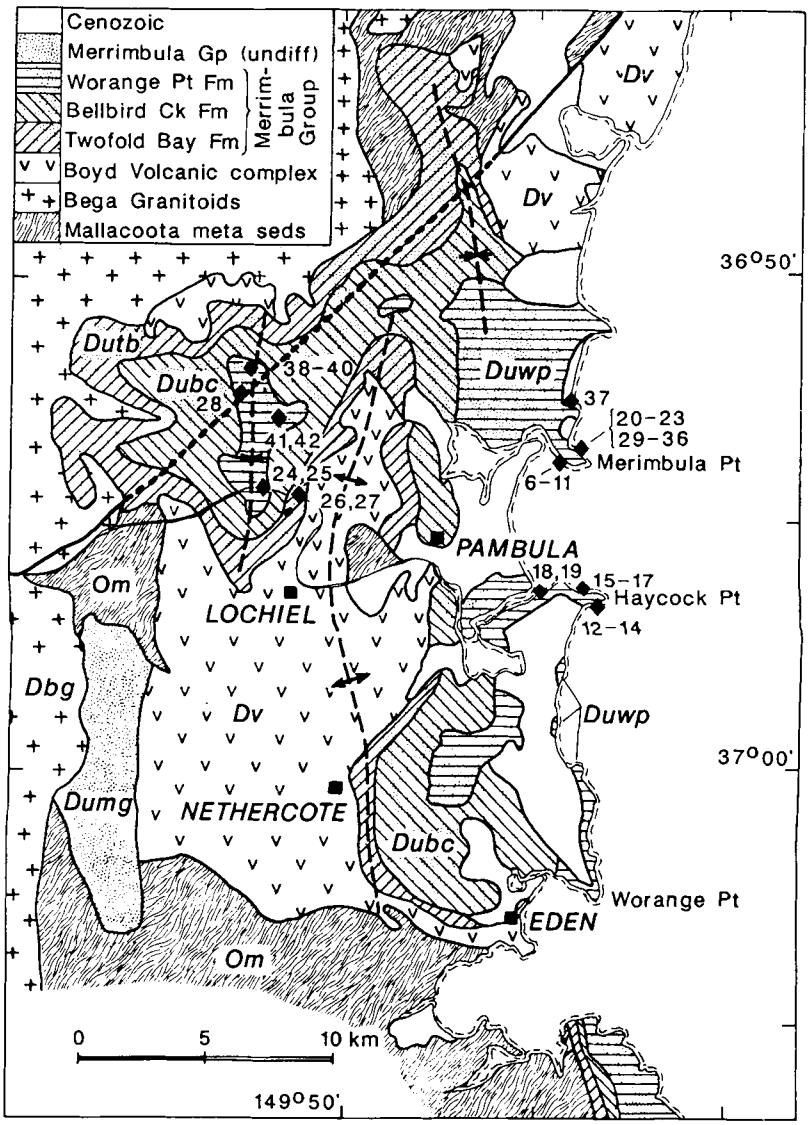

Figure 4. Geologic map of the Merimbula region of the New South Wales south coast (adapted from Steiner 1975; Fergusson *et al.* 1979; Powell 1983). Solid diamonds mark localities sampled; numbers are palaeomagnetic sites. WP on Fig. 1 shows the location of this map. Merrimbula Formation retains the original spelling, but the geographic names have been changed to Merimbula (Rixon *et al.* 1983).

A detailed sedimentological study of part of the Worange Point Formation by Taylor & Mayer (1990) describes seven distinct facies that comprise the interchannel and overbank deposits of an upward-fining fluvial cycle. Red mudstone floodplain deposits, which are terminated by an erosional surface, form the top of each fluvial cycle. This facies comprises about 20 per cent of lower parts of the formation, but nearly 50 per cent of upper parts; portions of the mudstone facies in lower parts were probably eroded by laterally migrating channels. The thickness of a complete cycle ranges from a few metres to more than 30 m; the average is about 10 m. Taylor & Mayer (1990) estimate that the recurrence time for the fluvial cycles is less than 10 000 yr. The thickest measured section in the Worange Point Formation is ~900 m (Powell 1983). Thus, the thickest section is estimated to represent deposition spanning roughly one million years.

The origin of the red colour, which is due to haematite, is pertinent to speculation on the depositional environment as well as the acquisition of magnetization. Steiner (1975) noted a correlation between colour and palaeocurrent direction, and advocated that the primary detritus was red. He considered the drab to greenish colour of the Bellbird Creek Formation (Figs 4 and 5) to be a consequence of progressive reduction in a paralic environment. The occurrence of rip-up clasts of the red mudstone within drab-coloured channel sand deposits suggests that the mudstone was red when redeposited, but the mudstone could have acquired its red colour after initial deposition. The correlation between palaeocurrent direction and colour could be a consequence of a correlation between palaeocurrent direction and depositional environment. The haematite in the Merrimbula Group sediments is probably a consequence of oxidation during prolonged subaerial

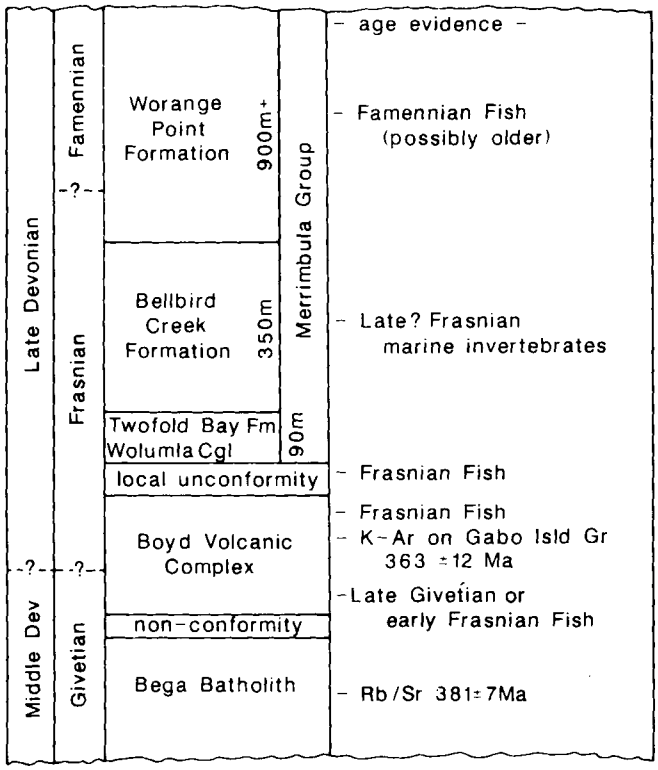

Figure 5. Schematic representation of regional stratigraphy and age evidence (after Fergusson *et al.* 1979). The K–Ar age on the Gabo Island Granite seems to be a minimum.

exposure as well as authigenic alteration associated with diagenesis (McIlveen 1975; Walker, Larson & Hoblitt 1981). Sand-filled desiccation cracks in the middle of the Worange Point mudstone units, and colour mottling, vermicular calcite glabules, and pseudoanticlines towards the top are pedogenic features representative of lower horizons of palaeosols (Taylor & Mayer 1990; Rixon, Bucknell & Rickard 1983).

Deposition of the Merrimbula Group began in middle or late Frasnian and probably ended in the Fammenian. Fossil evidence that bear on age of the Worange Point Formation is summarized by Young (in appendix to Fergusson *et al.* 1979). Remains of Placoderm fish (*Remigolepis* and *Groenlandaspis*) in the Worange Point Formation can be correlated with an uppermost Devonian sequence in Greenland, which is regarded as late Famennian or younger. In Australia, however, these fauna range down into the Frasnian. Marine invertebrates and palynomorphs in the Bellbird Creek Formation, which underlies the Worange Point Formation are no younger than Frasnian. Following folding during the mid-Carboniferous Kanimblan orogeny, the Merrimbula Group was succeeded by Permian rocks of the Sydney Basin (Powell 1983; McIlveen 1975). Thus, although the upper age limit is constrained strictly only by the folding, on the basis of the faunal assemblages Fergusson *et al.* (1979) inferred the Worange Point Formation deposition to be Frasnian to Famennian. An upper age limit of Famennian is consistent with the findings of continued palaeontological investigation of the Worange Point Formation (Robert Jones, Australian Museum, personal communication, December 1989).

Mild deformation of the Merrimbula Group is expressed as kink-like monoclines, conjugate box folds, and zonally developed solution-transfer cleavage. The deformation is a consequence of roughly horizontal, east–west compression, and accordingly, fold axes trend generally north–south. Deformation occurred under dilational conditions and, especially in shear zones, the fluid pressure was high. The monoclinal fold style is suggested to be a consequence of the thin-skinned nature of the strata being deformed. The overburden in the Merimbula* area perhaps never exceeded 1 km. Further north, where the Merrimbula Group is considerably thicker, the folds are more typical upright, rounded folds with well-developed slaty cleavage in the mudstone layers (Rixon *et al.* 1983).

A ubiquitous incipient cleavage in the sandstones consists of anastomosing seams with concentrations of white mica and haematite. In the mudstones and some siltstones a sub-vertical axial-planar slaty cleavage is well developed in tight hinges and steeply dipping limbs of folds. In thin section, both the incipient and slaty cleavage zones show strong alignment of mica flakes, elongation of quartz grains, and presence of seams of iron oxides (Rizon *et al.* 1983). Quartz–mica ratios indicate a reduction of 12–35 per cent of quartz in the cleavage seams in the sandstones. Spacing of the seams varies from a few centimetres to 30 cm in fine to coarse grained sandstone respectively. Because the spaced cleavage is perpendicular to bedding, even in steeply dipping limbs of folds, and is present in flat-lying beds distant from any fold hinges, it must be a consequence of layer-parallel shortening prior to folding (Rixon *et al.* 1983).

An estimate of the layer-parallel shortening within flat-lying strata can be based on the volume reduction in the spaced cleavage seams. Rixon *et al.* (1983) calculated that the maximum bulk shortening due to solution removal is about 1 per cent; and because the spaced cleavage is folded, this strain occurred prior to folding. Most of the pre-folding, layer-parallel strain was accommodated by the production of spaced cleavage. The monoclinal kink folds have a parallel to concentric style in the sandstone beds, but significant hinge thickening occurs in some mudstone layers. Slickensides on bedding-parallel quartz veins near fold hinges indicate that much of the folding took place by bedding-plane slip. The folding is estimated to have accommodated 5–10 per cent of shortening. Although shortening of 50–65 per cent is indicated in zones of concentrated cleavage, such high stain zones represent a small proportion of the rock, and Rixon *et al.* (1983) estimate the total strain to be less than 10 per cent.

PALAEOMAGNETISM

Sampling and laboratory methods

A palaeomagnetic site (e.g. McElhinny 1973) is a geologic unit, such as a single lava flow, that represents only a glimpse of geologic time. Primary remanent magnetism of a site provides a spot record of secular variation of the geomagnetic field. It is important to attempt to maintain a distinction between spatial and temporal distribution of a

* Since the naming of the Merrimbula Group, the spelling of the town has changed.

collection for palaeomagnetic analysis: the term 'site' should be used for reference to the representation of time, and 'locality' should be used to describe geographic distribution. Hence, several sites can be collected from the strata at one sea cliff locality; on the other hand, samples collected at several localities in one horizon, one thin lava flow, or one narrow dike, would all belong to the same site. In this study a site is a narrow sedimentary horizon representing a relatively short-lived episode of deposition. We collected five to 10 core samples from 37 sites (Fig. 4); a total of 228 samples. The samples collected at one site generally span less than a metre of section, but often cover several metres parallel to bedding. The cores were oriented both by magnetic and sun compass. We avoided sampling rocks with a pronounced cleavage.

In the laboratory the cores were sliced into standard palaeomagnetic specimens. Generally, only one specimen per sample was selected for study. The bulk susceptibility and low-field anisotropy of magnetic susceptibility (AMS) were measured for a few specimens from each site. After measurement of the natural remanent magnetization (NMR), most specimens were soaked in warm dilute HCl acid for about half an hour in order to remove any ferrous metal scraped from the drill or saw blade, and to investigate the effect of removing some of the surficial haematite pigment. After measurement of magnetization following the acid treatment, to lessen the contribution of any spurious IRM components associated with lightning strikes, most samples were demagnetized in an alternating field of 10–15 mT (100–150 Oe) and remeasured. Then, repeatedly, each specimen was heated, cooled in a less than 10 gamma environment, and remeasured. The temperature increments ranged from 200 °C at low temperatures to as little as 3 °C above 660 °C. The total number of heating increments for each specimen ranged from 8 to 22; the average was about 15. Heating was done in air, and the peak temperature for each step was maintained for ~20 min. For several specimens, acquisition of isothermal remanence up to 10 000 Oe, and continuous measurement of bulk susceptibility between −190° and 710 °C were investigated. Most of the measurements were done in the CSIRO (Commonwealth Scientific and Industrial Research Organization) rock magnetism laboratory in Sydney with an automated CTF cryogenic magnetometer. A subset (~8 per cent) of the collection was analysed in the palaeomagnetic laboratory at the Lamont–Doherty Geological Observatory in Palisades, New York.

Orthogonal projections of vector endpoints illustrating behaviour with incremental demagnetization were plotted for every specimen. Principal component analysis (PCA, Kirschvink 1980) was used to calculate the vector components from the incremental demagnetization data. For some specimens the PCA was done in an automatic mode, and for others steps were chosen by inspection of the vector endpoint graphs. Standard statistics for directional data on a sphere (Fisher 1953) were used to calculate site mean directions. Because VGPs commonly have a more nearly Fisherian distribution than directions (e.g. Cox 1970; Baag & Helsley 1974; Harrison 1980), the resultant palaeomagnetic pole is calculated from VGPs derived from directions. An analysis incorporating demagnetization planes (McFadden & McElhinny 1988), which is discussed in a later section, was applied in an attempt to obtain a better estimate of the sought-after characteristic direction.

Discussion of results

The NRM directions of the samples from most sites are generally upward and moderately scattered. The mean NRM intensities at a site range from 0.54 to 4.5 mA m^{-1} (5.4×10^{-7} to 4.5×10^{-6} emu cc^{-1}). An exception is Site 22, which has iron pisolites; NRM intensities from this site exceed 100 mA m^{-1} (1×10^{-4} emu cc^{-1}). The mean NRM intensity for each site is listed in Table 1. Bulk susceptibility ranged typically between 5 and 15 uG Oe^{-1}. The anisotropy of magnetic susceptibility (AMS) fabric is generally poorly defined, but the relatively well-defined site-mean poles to AMS fabric (minimum axes of susceptibility) are close to poles to bedding (Fig. 6).

The incremental thermal demagnetization experiments (Fig. 7) reveal that the magnetization is dominated by a consistent, well-defined, steep-upward-north component that post-dates the mid-Carboniferous folding (Fig. 8, Tables 1 and 2). It is gradually unblocked between 200° and 500 °C, but persists in many samples to higher temperatures. The unblocking temperature range and low bulk susceptibility indicate that the dominant magnetic carrier is haematite.

Isothermal remanence (IRM) acquisition experiments were done on several samples to test for the presence of magnetite (see Fig. 9). The increase in acquired IRM up to the peak field of 10 kOe is expected for haematite. The shallow slope of the initial segment of the IRM acquisition curve (before 1 kOe), indicates that magnetite, or any other low-coercivity magnetic mineral, is not present even in trace amounts (e.g. Dekkers & Linssen 1989; Dunlop 1972). Concentration of magnetite, with respect to haematite, as little as 0.1 per cent could be detected easily. Nearly constant bulk susceptibility between 500° and 650 °C in the two K–T experiments (one sandstone, one mudstone) also indicates that magnetite is not present. Although magnetite is present in rocks of the provenance, apparently all titanomagnetite or magnetite grains have been completely oxidized to haematite (e.g. Walker *et al.* 1981).

A characteristic component of magnetization is isolated between ~660° and ~680 °C in ~30 per cent of the specimens that were demagnetized (Figs 7 and 10, Tables 1 and 3). It is particularly well defined in a few mudstone samples. In 35 per cent of the sites, a characteristic component is defined satisfactorily by three or more specimens. The site-mean results are given in Table 3 and shown in Fig. 10. Both polarities are represented. For the several sites that have samples with characteristic components of both polarities, the majority polarity is adopted for the site mean. Statistical comparison between the two polarity subsets (McFadden & Lowes 1981), which are ~10° from being antipodal (Fig. 11, Table 4), shows that they are distinct at less than 50 per cent confidence.

The departure of the polarity subsets from antipodality is probably a consequence of incomplete removal of secondary components: i.e. failure to isolate truly univectorial components. Because the partial overprint direction is exclusively of normal polarity and steeper than the characteristic component, contamination of the characteris-

Table 1. Palaeomagnetic data from the Worange Point Formation.

			Characteristic Component Site Means									Secondary Component Site Means									
						uncorrected		corrected for tilt		VGP					uncorrected for tilt		VGP	corrected			
	Site	Pol	N/N_o	a95	k	Dec	Inc	Dec	Inc	Long(E)	Lat(N)	N/N_o	a95	k	Dec	Inc	Long(E)	Lat(N)	Dec	Inc	dp/dpaz	NRM J
1)	6	R	5/9	22.5	12.5	217.5	33.3	209.9	39.5	38.9	-60.4	9/9	5.3	97.0	336.9	-74.4	353.9	62.0	310.4	-66.6	12/93	1.07
2)	7	R	5/7	9.9	60.6	181.5	50.9	167.3	49.1	269.4	-77.4	7/7	8.4	52.0	345.7	-70.7	353.7	69.4	320.2	-64.5	12/93	0.87
3)	8	N	6/7	3.2	447.6	0.8	-56.3	350.5	-49.9	95.3	80.0	4/5	poorly defined, scattered secondary component								10/125	2.43
4)	9	N?	0/10									6/6	8.5	62.9	310.3	-71.5	13.3	51.9	52.6	-81.6	22/288	1.86
5)	10	N?	0/7									5/5	9.3	68.0	28.3	-83.7	321.2	47.6	85.5	-73.7	14/288	2.76
6)	11	B	4/10	17.5	28.4	8.5	-60.0	8.5	-60.0	273.6	82.3	8/9	11.1	26.0	349.0	-80.4	336.0	55.1	349.0	-80.4	0/0	2.35
7)	12	B	6/10	23.8	8.8	190.8	53.4	217.8	33.9	41.3	-52.2	7/8	7.1	72.3	356.8	-70.1	336.2	72.7	48.2	-50.1	33/260	0.84
8)	13	N	3/7	13.7	82.1	350.4	-53.4	17.1	-42.1	204.0	70.7	5/6	12.6	37.6	329.0	-73.4	1.8	60.1	32.1	-62.0	26/249	2.58
9)	14	B	0/7									6/6	8.4	63.9	340.4	-66.5	13.4	71.3	320.2	-53.7	17/108	1.08
10)	15	N	4/8	13.6	46.3	359.5	-62.2	46.2	-39.3	232.9	47.7	6/6	9.5	51.1	33.8	-85.9	323.6	43.5	78.5	-46.3	41/263	3.24
11)	16	B	4/6	32.1	9.2	239.4	38.2	234.4	43.8	62.3	-42.8	6/6	10.7	40.3	6.6	-59.6	276.4	83.8	353.8	-57.8	8/103	0.98
12)	17	B?	0/7									7/7	9.1	44.6	0.2	-74.5	329.7	65.9	38.7	-71.3	12/275	1.34
13)	18	B	0/11									9/9	8.1	41.6	359.5	-60.3	334.9	85.6	288.1	-44.2	50/68	0.64
14)	19	B	0/7									6/7	6.6	104.3	333.4	-63.8	28.3	68.4	307.8	-62.1	13/58	1.24
15)	20	R	2/10									7/7	7.6	63.4	4.1	-63.6	310.8	81.1	347.2	-68.8	9/51	0.76
16)	21	B	2/7									5/6	11.1	48.7	358.1	-70.4	333.5	72.3	328.4	-73.6	10/55	2.14
17)	22	B	0/6	pisolites with multiple antipodal components								5/6	9.3	68.5	357.3	-62.3	346.1	83.0	338.0	-66.2	10/55	26.89
18)	23a32a	R	6/8	7.0	91.5	208.2	27.5	202.9	30.0	20.3	-61.0	8/8	6.2	81.5	335.0	-72.4	359.5	63.0	316.7	-65.2	10/101	2.35
19)	23b	B	0/4	sandstone filling in mudcracks of previous site								4/4	8.2	125.8	19.1	-77.1	315.2	59.1	338.9	-74.9	10/101	1.40
20)	24	B	0/5	overlapping antipodal components								4/5	14.3	42.3	312.8	-81.7	347.3	46.8	84.1	-62.2	34/275	1.36
21)	25	R	0/5									4/4	anomalously low coercivity								34/275	0.84
22)	26	R	2/6									5/5	6.6	137.3	61.8	-83.6	314.8	42.0	95.5	-42.9	42/281	1.48
23)	27	R	1/3									2/3									46/289	4.50
24)	28	R	2/7									6/6	7.3	85.3	0.7	-76.9	329.2	61.9	60.8	-80.1	12/314	1.18
25)	29	B	0/4									3/3	15.2	66.6	26.6	-63.4	270.2	68.5	55.1	-41.4	30/266	1.84
26)	30	R	0/3									3/3	12.3	101.3	83.8	-71.6	288.7	33.2	85.0	-41.6	30/266	0.54
27)	31	B	0/3									3/3	8.0	237.0	50.6	-69.6	281.8	51.7	70.2	-42.1	30/266	1.80
28)	33	B?	0/6									4/6	12.4	56.1	64.0	-70.1	283.0	43.8	85.4	-31.6	46/280,28/270	3.68
29)	34	N?	0/5									5/5	10.7	52.4	55.5	-69.6	281.6	48.8	78.9	-52.6	28/270,15/326	1.29
30)	35	B	3/8	21.2	34.7	189.9	20.6	183.5	10.4	336.5	-58.2	7/7	7.2	70.9	24.2	-66.3	281.4	68.8	36.3	-51.3	8/228,28/240	1.63
31)	36	B	0/10									10/10	8.9	30.2	8.4	-67.3	310.1	73.2	43.5	-68.2	28/301, 2/71	4.58
32)	37	R	6/6	19.6	12.7	196.0	19.7	198.8	18.8	6.6	-57.9	5/6	16.7	21.8	21.5	-74.6	307.6	62.2	45.9	-71.5	8/281	1.08
33)	38	B?	0/5									5/5	7.2	112.6	0.1	-62.9	329.2	82.6	13.0	-34.7	30/208	0.96
34)	39	N	0/4									4/4	14.1	43.4	13.0	-59.4	261.8	79.3	19.2	-30.0	30/208	1.64
35)	40	B	7/17	14.7	17.8	173.6	65.9	189.5	49.2	21.8	-79.6	8/8	10.0	31.7	12.6	-49.9	212.8	77.8	20.6	-34.6	30/198,19/317	1.86
36)	41	B	0/6									5/5	15.0	26.9	8.4	-76.4	321.9	62.3	41.5	-33.7	46/233	0.75
37)	42	N	4/5	7.8	138.0	20.0	-56.3	34.8	-28.1	213.7	52.1	4/4	10.8	72.8	342.8	-63.6	21.7	74.6	20.4	-44.1	32/237	2.23

Central Location: 149.9E 36.9S

Explanation of Table 1 Headings:

Site: Each site is a sedimentary horizon

Pol: Polarity of characteristic component: N (normal); R (reversed); B (both polarities present).
majority polarity used for mean site result

N/N_o: N is the number of specimens that comprise the site mean; N_o is the number of specimens demagnetized;
in a few instances two specimens from the same sample were demagnetized.
A site mean is calculated if a component is defined satisfactorily in more than 2 specimens per site.
For sites with varying attitudes, the a-95 and k pertain to the tilt corrected result.

a-95: alpha-95; at the 95% confidence level the true mean lies within a circle of radius a-95 about the site mean result.

k: proportional to concentration of the data; $k = N-1/N-R$; R is the magnitude of the vector sum of N unit vectors.

Dec Inc: Declination and Inclination of site-mean direction (in degrees), before and after correction for tilt of bedding.

VGP: Virtual Geomagnetic Pole postion calculated from the tilt-corrected site-mean characteristic direction,
and uncorrected site-mean secondary direction

dpaz/dp: azimuth of the dip direction, and the dip (in degrees).

NRM J: Mean NRM intensity for the site times 10e-6 emu/cc.

tic component by a residual secondary component will give the normal polarity results a steep bias, and the reverse polarity results a shallow bias. The residual secondary component is more difficult to detect when superimposed on a normal polarity characteristic component than on a reversed one, so the overprint bias is probably less for the reverse polarity results than for the normal results. Moreover, dispersion of the normal polarity characteristic component data upon correction for tilt indicates that the contribution of residual post-folding components is significant. In fact, the subset of normal polarity site-means fails a 'fold test' at a high confidence level (Fig. 10, Table 4). Thus, the reverse polarity subset mean result is more reliable than the whole data set.

Because the characteristic magnetic direction lies at a small angle from the fold axes, the 'fold test' applied to all

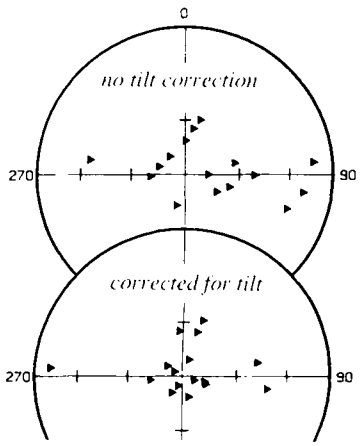

Figure 6. Poles to planar fabric defined by anisotropy of magnetic susceptibility (AMS). Each pole is a Fisher mean of the minimum axis of susceptibility measured in several samples from one site. Only poles with α_{95}s less than 30° are shown. Cluster about vertical after application of tilt corrections demonstrates that the AMS fabric is generally parallel to bedding. The three discordant sites with shallow poles (13, 24, 34 from left to right) do not have satisfactorily defined characteristic remanent magnetization.

the reverse polarity characteristic data is inconclusive. At one locality, however, despite rather dispersed and poorly defined characteristic directions, two sets of samples from opposite limbs of a local syncline pass a fold test at 90 per cent confidence (Fig. 12). Moreover, the results from 10 specimens that are used as 'set points' in the great circle analysis (discussed below) because they have the highest quality definition of a characteristic component, pass a fold test at greater than 95 per cent confidence (Fig. 13).

Although the high-temperature component seems to predate the mid-Carboniferous folding, the presence of both polarities in individual sites indicates that the magnetization was acquired over a considerable period of time. A sedimentological study and hydrological model of the Worange Point Formation deposition indicates that palaeosol features took on the order of ten thousand years to develop (Taylor & Mayer 1990). It is plausible that remanent magnetization was acquired over a similar range of time during oxidation associated with palaeosol development. Remanence could also have been acquired later as a consequence of dehydration reactions associated with prolonged weathering (e.g. Idnurm & Schmidt 1986) and the early stages of diagenesis. Haematite that formed during the early stage of deformation may also contribute substantially to the remanent magnetization. The absence of magnetite is indicative of an advanced degree of oxidation which typically takes millions of years to attain (Walker *et al.* 1981).

A prolonged period of acquisition of remanent magnetization complicates the definition of a 'palaeomagnetic site'. If samples from one horizon have antipodal magnetic directions, clearly an appreciable record of secular variation is averaged. Accordingly, irrespective of the duration of the deposition of the horizon, the remanent magnetization of the horizon does not represent a discrete 'palaeomagnetic site'. Because it is clear that the magnetization of the Worange Point Formation was acquired over a protracted period, it is valid to treat each specimen as a site. However, the results are also presented in conventional fashion: retention of the original geological site designation (Fig. 10, Table 3). A third method of analysis, great circle analysis, utilizes information from some of the demagnetization experiments that fail to isolate a stable component.

Great circle analysis

Only ~30 per cent of the Worange Point demagnetization experiments provide acceptable isolation of a characteristic component, and most of the definitions of a characteristic component are of marginally adequate quality. However, the incremental demagnetization experiments that do not reveal a characteristic component, often have a series of directions defined by the intermediate to high temperature demagnetization steps that is roughly coplanar and trends toward the vicinity of the mean direction determined from specimens that do reveal a characteristic component. The demagnetization planes can help to constrain the direction of the characteristic component.

If incremental demagnetization defines a series of vectors that consist of a varying ratio of two components, the vectors will be coplanar; on a stereonet the directions will lie along a great circle. Consider an example where components I and II were acquired before and after folding respectively. If samples are collected from strata of widely varying attitude, then without compensation for tilt, component II in all the samples will be nearly colinear, but component I will be dispersed; the great circle demagnetization paths will intersect at the component II direction. On the other hand, with compensation for tilt, the component Is will be colinear and the IIs will be dispersed; the great circle demagnetization paths will intersect at the component I direction.

The intersecion point of great circles is an accurate estimate of a component, only if, in the chosen reference frame, the dispersion of the other component is much greater (e.g. $k_{II}/K_I \lesssim 0.1$; Schmidt 1985; see Fig. 14a). In the chosen reference frame, if the dispersion of one component is markedly less than the other, the mean of the low dispersion component is a pole to the plane (great circle) that is fitted to the poles of the demagnetization great circles. If the dispersion of the two components is too similar, then the plane will be a compromise between two planes: one with component I as a pole the other with component II (Fig. 14b). Hence the potential bias in the accuracy of the intersection of demagnetization great circles.

We have applied a method of analysis (McFadden & McElhinny 1988) that combines reliable stable endpoint characteristic component determinations ('set points') with information provided by the demagnetization experiments that do not isolate a characteristic component, but define great circles. For each great circle, 'sector constraints' are chosen to delimit an arc segment within which it is reasonable that the undetermined characteristic direction lies. 79 of the Worange Point incremental demagnetization experiments were judged by visual assessment of orthogonal vector endpoint diagrams and stereonet plots of directions to have well-defined great circle paths. All are great circle paths that trend toward a characteristic component of reversed polarity; the normal characteristic component data have inadequately defined great circle paths because an arc

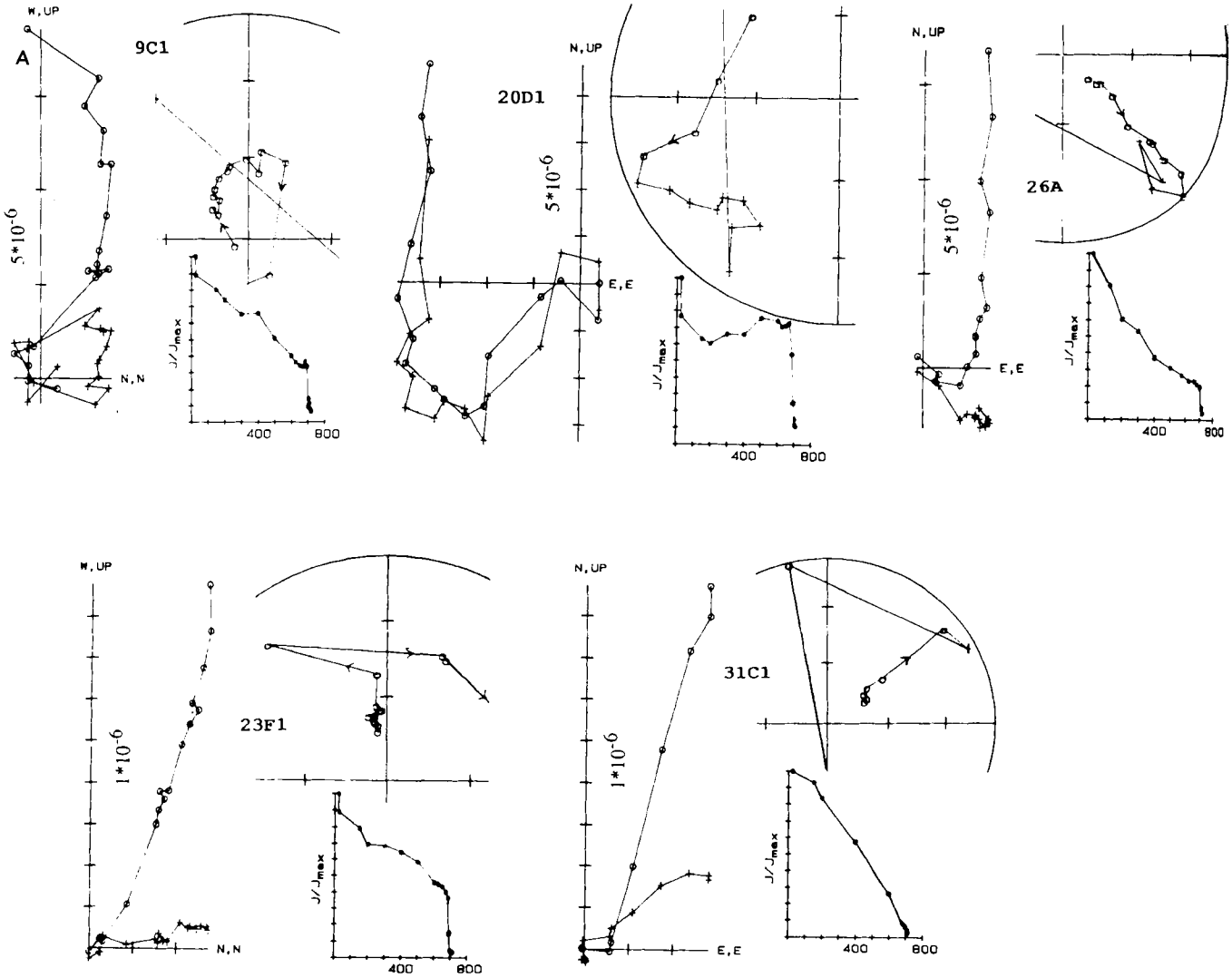

Figure 7. Orthogonal projections of vector endpoints showing representative results of incremental, thermal demagnetization experiments on Worange Point Formation specimens. 'o' = projection on vertical plane; ' + ' projection on horizontal plane. Numbers along axes of orthogonal projections are values of one division on the axis in emu cc^{-1}. (A) Examples of clear definition of the steep secondary component, and poor or no isolation of a stable characteristic component. (B) Examples of possible isolation of the normal polarity (NE–upward) characteristic component. Often, however, the steep normal overprint and the characteristic normal components overlap, so positive identification of a characteristic component is difficult (e.g. specimen 15D2). (C) Examples of adequate isolation of a reversed polarity (SW–downward) characteristic component.

between the secondary and normal polarity characteristic component subtends only ~25°.

Poles to best-fit great circle demagnetization paths were calculated by principal component analysis (e.g. Kirschvink 1980) of a series of unit-vector endpoints with the plane anchored to the origin. Each series of demagnetization steps to which a plane was fitted, and the approximate endpoints to an acceptable segment of the great circle, were chosen by visual assessment of the plots of demagnetization data. Results from the specimens with high-quality definition of an isolated characteristic component were used as 'set points' that are pooled with the great circle data. The demagnetization data from 10 of the 40 specimens with a reversed characteristic component were judged by visual inspection to be of sufficient quality for 'set points'. Excluding the set-point great circles and seven outliers reduced the number of great circles to 62. The great circle analysis data are shown in Fig. 15. The mean direction determined by the McFadden & McElhinny (1988) great circle analysis technique is ~10° steeper than that determined without incorporation of the great circle data. Fig. 16 shows a comparison of the mean results determined by different methods.

Is the great circle analysis result a better estimate of the characteristic remanent magnetization direction? To explain the discrepancy between the great circle analysis and the conventional estimates of the mean characteristic component, one might suggest that even when isolation of a reversed characteristic component was judged adequate, some of the steep normal secondary component remains, resulting in a direction that is too shallow. If so, the great circle analysis result, if it is closer to the true characteristic

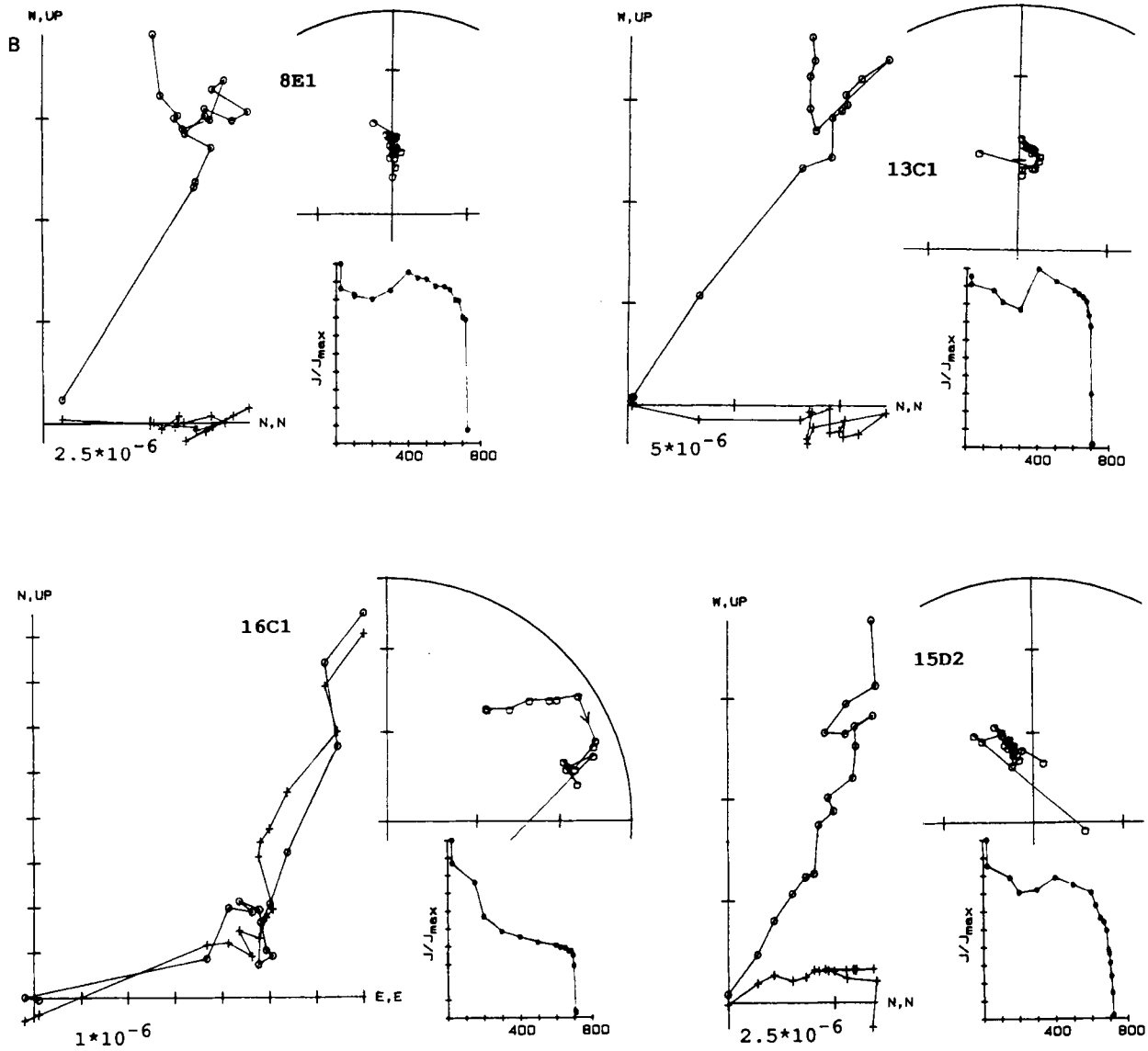

Figure 7. (*continued*)

direction, would be steeper. However, bias in the great circle analysis due to insufficient difference in the dispersion of the characteristic and secondary components in stratigraphic coordinates (i.e. compensated for tilt of bedding) would cause the estimate of the characteristic component, in this case, to be too steep. And in geographic coordinates (i.e. without tilt corrections), assuming that inadequate contrast in dispersion is due to insufficient attitude variation, the great circle analysis estimate of the secondary component should be too shallow. Although a complete application of the McFadden & McElhinny (1988) method of great circle analysis was not done for the secondary component, an estimate of the secondary component given by the pole to the plane that is fitted to the poles to demagnetization great circles (in geographic coordinates) is more than 14° too shallow (see Fig. 16).

The bias problem inherent in analyses of intersecting demagnetization planes can be lessened by constraining each estimate of a characteristic component to a specified sector of each great circle (McFadden & McElhinny 1988), but to overcome a potentially significant bias problem, the sector constraints must be tight. Sufficiently strict constraints, however, can only be justified if the sought-after characteristic component is *a priori* well determined by set points, in which case the great circle analysis is probably of little value. McFadden and McElhinny mention that the 'overall result is quite insensitive' to the subjective great circle sector constraints. The sensitivity, however, is related to the number of best estimate directions that are actually pinned by the sector endpoints. If, after the final iteration, no best estimate points on the great circles fall outside the sector constraints, then, without the set points, the resultant maximum likelihood estimate of the sought-after characteristic direction is nearly identical to the result given by the pole to the plane that is fitted to the poles to the demagnetization great circles (e.g. Halls 1976); the bias is no different (see Fig. 16). Thus, in practice, the sector constraints often cannot substantially reduce the bias due to insufficient contrast in dispersion of the populations of the two components.

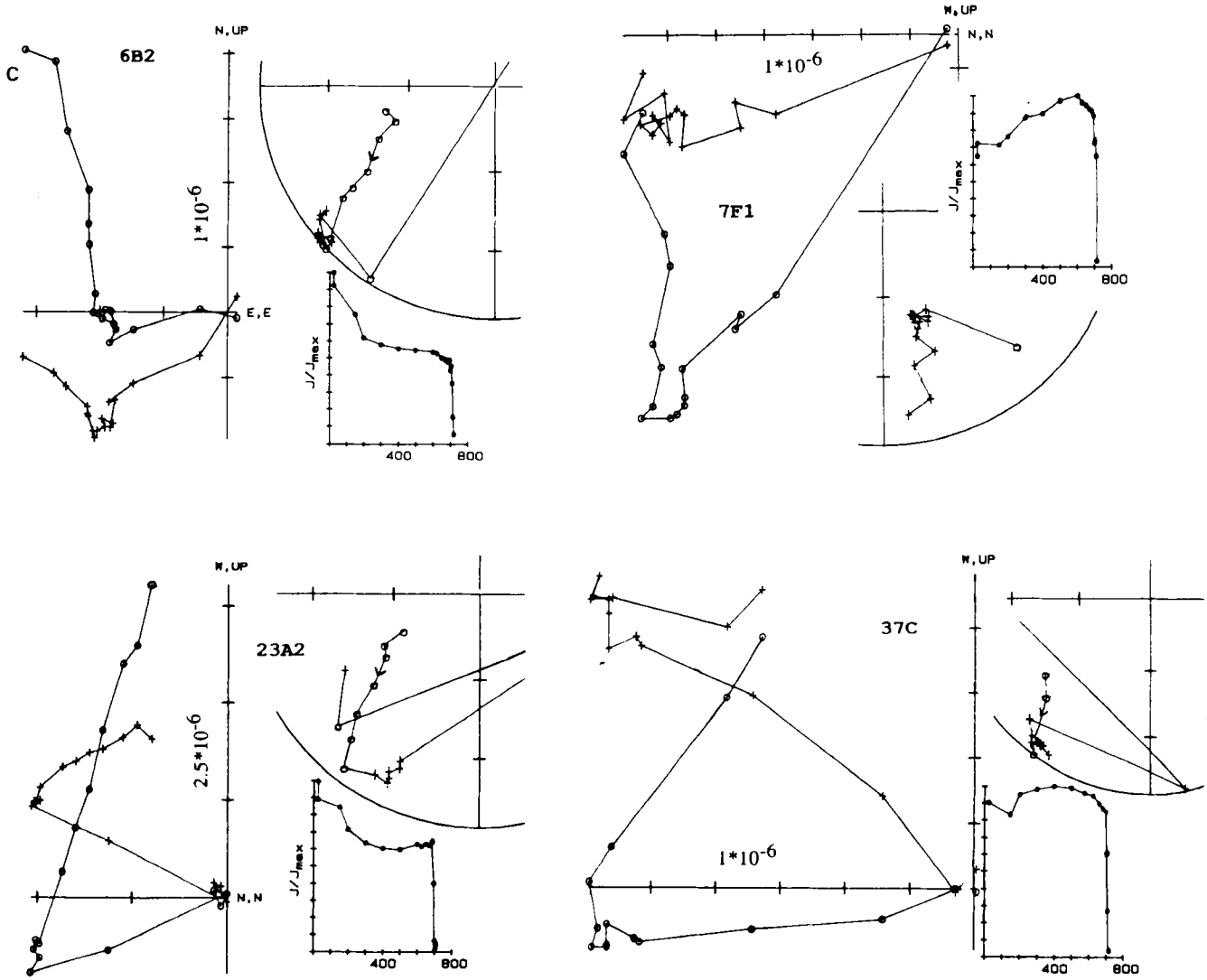

Figure 7. (*continued*)

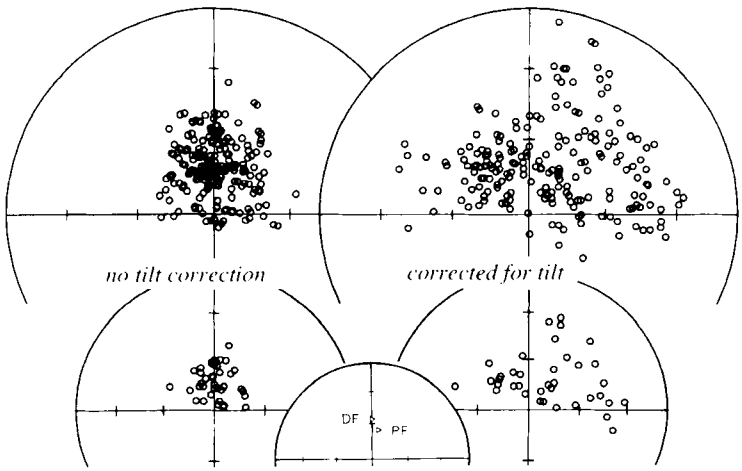

Figure 8. Magnetic directions that are removed at relatively low temperature. All samples (upper pair). Site means (lower pair). Dipole and present field (inset at bottom). The marked dispersion of directions after compensation for tilt, establishes that this component of magnetization post-dates the mid-Carboniferous folding. Open symbols are on the upper hemisphere, solid on the lower (none here). Equal area stereographic projections. Same for subsequent figures with stereonets.

Table 2. Secondary component mean results.

I. Site Means (Site data are given in Table 1)

Directions

	N/N_O	Dec	Inc	a95	k	R	sd	colat*
uncorrected for tilt:	34/37	5.6	-72.3	3.7	44.8	33.2635	12.1	32.5
corrected for tilt:	34/37	30.8	-65.4	9.0	8.5	32.0614	19.6	31.4

South Poles (means of VGPs from site mean directions)

	N/N_O	Long(E)	Lat(S)	A95	K	R	sd	colat
uncorrected for tilt:	34/37	142.1	68.0	6.1	17.0	32.0614	19.6	31.4
corrected for tilt:	34/37	94.0	65.8	12.7	4.8	27.0684	37.1	39.1

II. Mean of Individual Specimens

(data excluded if fewer than 3 specimens per site produced satisfactory results)

Directions

	N/N_O	Dec	Inc	a95	k	R	sd	colat
uncorrected for tilt:	197/207	2.4	-71.6	1.9	27.6	189.9014	15.4	33.6
corrected for tilt:	197/207	21.8	-67.4	3.9	7.6	171.1212	29.4	39.8

South Poles (means of VGPs)

	N/N_O	Long(E)	Lat(S)	A95	K	R	sd	colat
uncorrected for tilt:	197/207	146.4	68.6	3.1	11.2	179.5655	24.2	31.7
corrected for tilt:	197/207	117.9	68.7	5.6	4.2	150.8197	39.3	36.3

*colatitudes from south pole

Only two of the 62 Worange point demagnetization great circle estimate points are affected in the final iteration by sector constraints. Thus, without including the 10 set points, the bias in the result of the McFadden & McElhinny (1988) method is essentially the same as it is for the great circle intersection point defined by the pole to a plane that is fitted to the poles to the great circles; the two differ by only 0.6°. The result, without the set points, is nearly 4° steeper than the great circle analysis that included set points and sector constraints. The latter is ~10° steeper than the original mean result of the conventional principal component analysis (see Fig. 16). The ~4° difference between the two great circle analysis results is attributable to the set points, not the sector constraints.

Using a range of estimates of the ratio of precision parameters for the low-temperature and characteristic components in stratigraphic coordinates (k_{II}/k_I), and the angular departure of the two components from antipodality, Schmidt's (1985) graphs of compiled estimates of the bias inherent in converging great circle methods predict a bias between 4° and 12° for the result of the great circle analysis of the Worange Point data without set points or sector constraints. The precision parameter of the low-temperature component (k_{II}) is well determined (Table 2). The conventional determinations of the characteristic component mean direction provide estimates both of the precision parameter of the characteristic component (k_I) and of the departure of the two components from antipodality (α). A reasonable range for α is 20°–30°. The bias analysis is most sensitive to the choice of k_I; k_I ranges from ~10 to ~16 (Tables 3 and 4), and for the 10 set points k is ~30. For the latitude that is indicated by the conventional characteristic mean result, a precision parameter of ~30 is consistent with a model of palaeosecular variation based on the Late Cainozoic geomagnetic field (Harrison 1980; Cox & Gordon 1984). The precision parameters for the great circle analysis

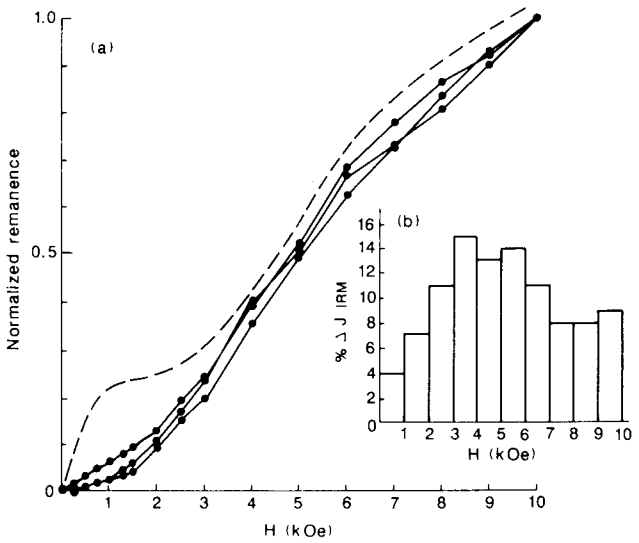

Figure 9. Acquisition of isothermal remanence (IRM). (A) Graph of applied DC magnetic field versus normalized remanence. Data points are plotted for a mudstone, a siltstone—very fine-grained sandstone, and a fine-grained sandstone from Sites 37, 38 and 12 respectively. Continuing increase in IRM acquisition up to the peak attainable field of 10 kOe is typical of haematite or goethite, but the high unblocking temperature rules out goethite. The absence of any shoulder near ~1 kOe, the field at which magnetite saturates, indicates that magnetite, titanomagnetite, or maghaemite are not present even in trace amounts. Concentrations of any such low-coercivity minerals of as little as 0.1 per cent, with respect to haematite, would cause an easily detectable rapid increase in IRM acquisition at applied fields less than 1 kOe. The IRM curve would have a low-field shoulder such as the dashed curve, an example from Dekkers & Linssen (1989) of haematite with a trace amount of magnetite contamination. (B) (inset) The corresponding coercivity spectra of the IRM acquisition.

and for the characteristic component site means are ~15. A k_1 of ~ 15 gives a bias estimate of ~8°.

The difference between the result of the great circle analysis without set points and the mean result without utilizing the great circles is ~13° (Fig. 16). Much of the discrepancy could be a consequence of bias in the great circle analysis (Schmidt 1985; see Figs 14 and 16). The inclusion of the set points in the great circle analysis reduces the bias, but the sector constraints do not unless they are unrealistically strict. If the precision parameter for the characteristic component (k_1) was known, then probably the best estimate of the sought-after mean characteristic direction would be to correct the result of the great circle analysis without set points for the predicted bias. However, because k_1 cannot be estimated accurately, the bias estimates range from 4° to 12°.

Best estimate of the palaeopole position

What is the best estimate of the mean direction of characteristic remanent magnetization and the corresponding pole position? A comparison of the mean results calculated in different ways is shown in Fig. 16. The result of the great circle analysis suffers from an indeterminable bias. However, as a consequence of the great circle analysis it was discovered that the set point data pass a fold test at greater than 95 per cent confidence. Indeed, the mean of the 10 set point specimens (Fig. 13), the highest quality data, may be the most reliable overall result. The fact that only 25 per cent of the reversed characteristic results were used for set points in the great circle analysis emphasizes that many of the demagnetization results used in the conventional analysis have only marginally acceptable definitions of an isolated characteristic component. Nonetheless, the close agreement between the set points result and results

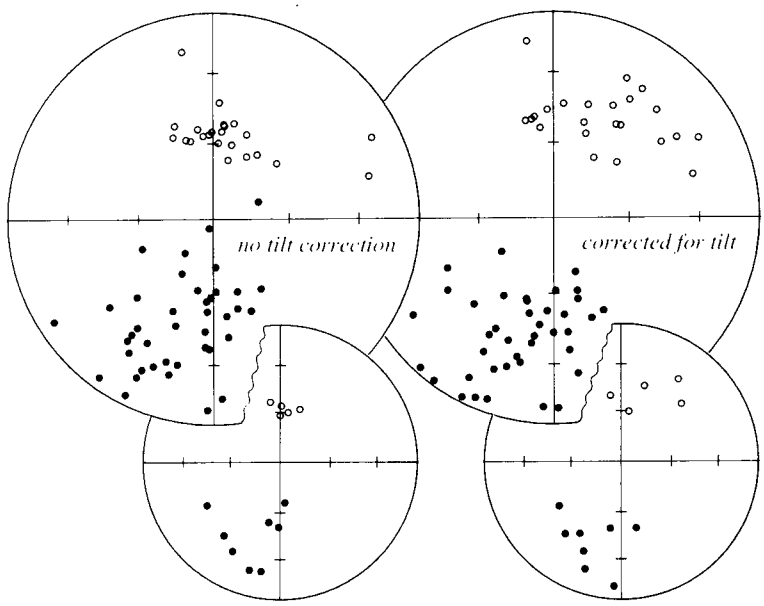

Figure 10. Magnetic directions that are isolated at high temperature (between ~600° and 680 °C): the characteristic component, which is well defined in only 47 per cent of the sites. Upper pair: all specimens from sites with three or more specimens with satisfactory definition of a characteristic component. Lower pair: site means. Note that the normal specimen directions are more dispersed after correction for tilt. Isolation of a stable characteristic component is clearer in the specimens with reverse polarity; the normal characteristic results are contaminated by an incompletely removed overprint.

Table 3. Characteristic component mean results.

(Reversed directions and poles inverted to normal antipodes)

I. Site Means (Site data are given in Table 1)

Directions

	N/N_O	Dec	Inc	a95	k	R	sd	colat*
uncorrected for tilt:	13/37	16.0	-47.6	10.9	15.4	12.2219	20.6	61.3
corrected for tilt:	13/37	21.1	-39.6	10.7	15.9	12.2459	20.3	67.5

South Poles (means of VGPs from site mean directions)

	N/N_O	Long(E)	Lat(S)	A95	K	R	sd	colat
uncorrected for tilt:	13/37	36.7	76.4	11.0	15.1	12.2054	20.8	59.3
corrected for tilt:	13/37	28.6	67.9	10.9	15.4	12.2198	20.7	66.4

II. Mean of Individual Specimens

(data excluded if fewer than 3 specimens per site produced satisfactory results)

Directions

	N/N_O	Dec	Inc	a95	k	R	sd	colat
uncorrected for tilt:	63/74	15.1	-47.9	5.9	10.3	56.9844	25.2	61.1
corrected for tilt:	63/74	20.2	-40.1	5.7	10.9	57.3327	24.5	67.1

South Poles (means of VGPs)

	N/N_O	Long(E)	Lat(S)	A95	K	R	sd	colat
uncorrected for tilt:	63/74	38.8	77.6	6.3	9.2	56.2450	26.7	58.3
corrected for tilt:	63/74	28.3	69.4	5.7	10.8	57.2839	24.6	65.5

*colatitudes from south pole

incorporating more data, indicates that the means of the larger data sets are reasonably accurate. As discussed, the reverse polarity characteristic components are more clearly isolated than the normal ones.

The overall result is calculated from the 40 specimens with adequate definition of a reverse characteristic component (Table 4): Dec. = 196.8°, Inc. = 38.1°, $\alpha = 7.4°$. The south pole position is derived from the specimen VGPs: 19.7°E, 70.8°S, $\alpha_{95} = 7.1°$. The mean of the site mean reverse characteristic directions gives a more conservative result (Table 4), but the timing of CRM acquisition bears no systematic relationship to the geological sites, so statistical treatment of the specimens independently is reasonable. Moreover, the mean of the reverse specimens is closer to the range of the bias-corrected result of the great circle analysis than the mean of site means. The error associated with the mean of reverse polarity specimens, however, is unrealistically small.

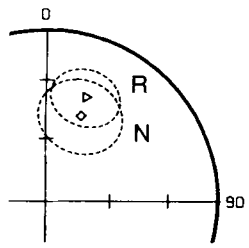

Figure 11. Reversal test: α_{95}s about the mean poles of normal and inverted reverse polarity subsets. Isolation of a stable characteristic component is clearer in the specimens with reverse polarity; the normal characteristic results are contaminated by an incompletely removed overprint.

IMPLICATIONS OF THE CHARACTERISTIC MAGNETIZATION

The palaeopole position indicated by the characteristic magnetization of the Worange Point Formation (Fig. 17) lies

Table 4. Reversal test of characteristic component.

(Site data are given in Table 1)
(Reversed directions and poles inverted to normal antipodes)

Directions

		N/N_O	Dec	Inc	a95	k	R	sd	colat	angle	% diff
					uncorrected for tilt						
Means of site-means	normal:	5/5	3.7	-58.0	6.6	134.9	4.9703	7.0	51.3	21.2	44
	reverse:	8/8	21.7	-40.2	16.0	12.9	7.4566	22.6	67.1		
Means of specimens	normal:	23/28	10.5	-54.4	8.4	14.0	21.4293	21.6	55.1	11.4	93
	reverse:	40/46	17.4	-43.9	7.8	9.3	35.8206	26.5	64.3		
					corrected for tilt						
Means of site-means	normal:	5/5	21.9	-45.6	18.8	17.4	4.7707	19.4	63.0	9.8	47
	reverse:	8/8	20.6	-35.8	15.0	14.5	7.5175	21.3	70.1		
Means of specimens	normal:	23/28	26.3	-43.4	8.9	12.5	21.2416	22.9	64.8	8.9	82
	reverse:	40/46	16.8	-38.1	7.4	10.4	36.2510	25.1	68.6		

VGPs (South Poles)

		N/N_O	Long(E)	Lat(S)	A95	K	R	sd	colat	angle	% diff
					uncorrected for tilt						
Means of site-means	normal:	5/5	94.3	86.5	9.1	71.7	4.9442	9.6	51.2	20	58
	reverse:	8/8	31.2	68.6	16.3	12.5	7.4422	22.9	65.2		
Means of specimens	normal:	23/28	54.7	82.5	9.4	11.3	21.0571	24.1	54.1	8.9	82
	reverse:	40/46	34.3	74.5	8.3	8.4	35.3470	28.0	60.9		
					corrected for tilt						
Means of site-means	normal:	5/5	38.4	70.6	21.1	14.1	4.7158	19.4	63.0	7.2	27
	reverse:	8/8	23.6	65.9	14.9	14.8	7.5269	21.1	69.2		
Means of specimens	normal:	23/28	40.6	66.1	9.8	10.5	20.9109	25.0	63.7	8.9	82
	reverse:	40/46	19.7	70.8	7.1	11.3	36.5356	24.1	66.6		

Explanation of Table 4 Headings:
see explanation to Table 1.
colat: colatitudes of the mean result from the south pole.
angle: the angle between the two polarity subset means.
% diff: ~max confidence level at which the two mean results are distinct (McFadden and Lowes, 1981)

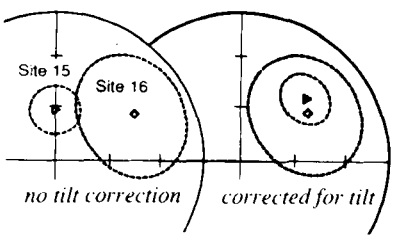

Figure 12. Fold test of results from Sites 15 and 16, which are from opposite limbs of a syncline. The sites are only ~60 m apart, and from similar stratigraphic levels. Ellipses are α_{95}s about the site means. The two site means are distinct at >90 per cent confidence before correction for tilt, but at <10 per cent after correction for tilt (McFadden & Lowes 1981).

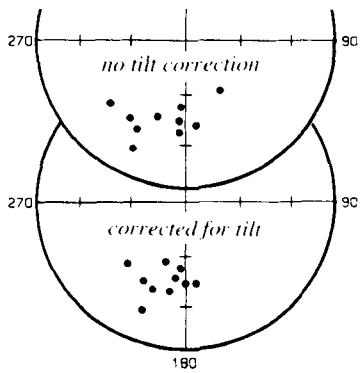

Figure 13. Characteristic directions from the highest quality demagnetization data, which are used as 'set points' in the great circle analysis. The improvement in precision with tilt correction constitutes a positive fold test at greater than 95 per cent confidence (McFadden & Jones 1981). The mean result : $n = 10$, Dec. = 195.1, Inc. = 43.0, $\alpha_{95} = 8.5$, $k = 33.2$. South pole derived from the corresponding VGPs: 22.0°E, 73.0°S, $\alpha_{95} = 9.0$, $K = 29.8$.

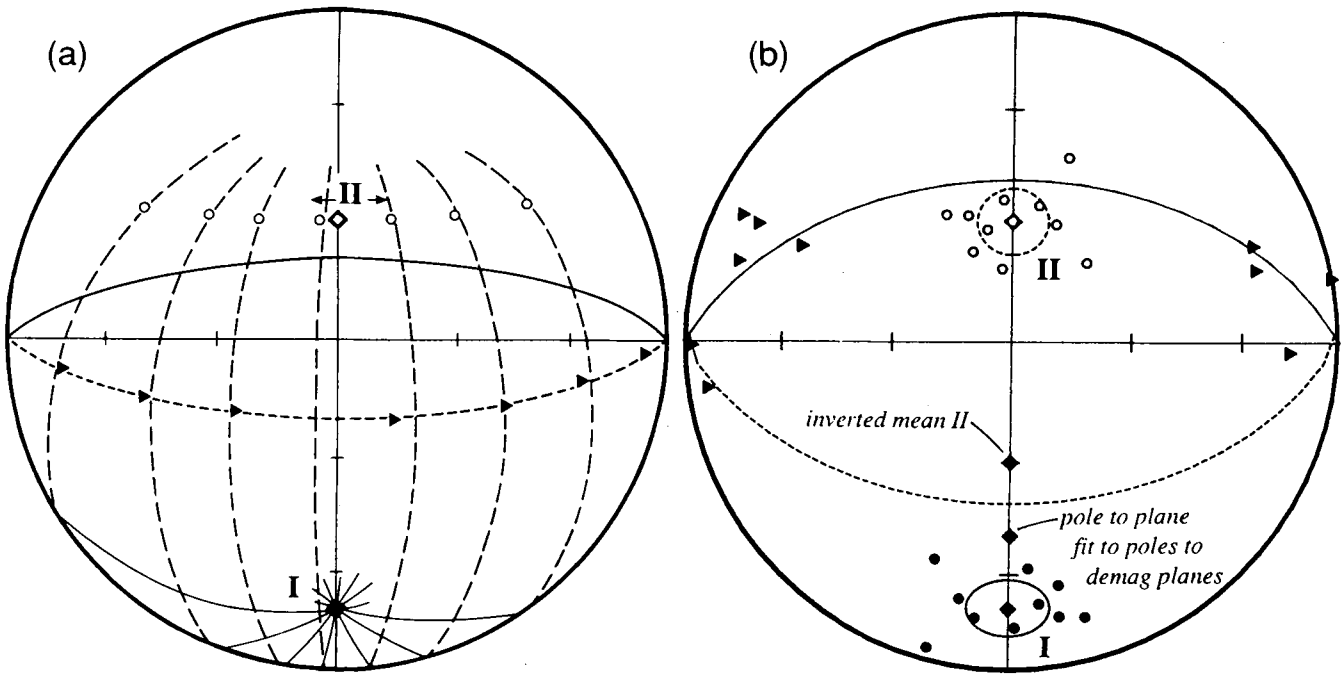

Figure 14. (A) Illustration of idealized great circle geometry. Components I and II were acquired before and after folding respectively. For the purposes of illustration, both have unrealistically high precision parameters. Variable tilt about north–south strike disperses C_{II}. In stratigraphic coordinates (tilt-corrected), demagnetization planes defined by varying ratios of C_I and dispersed C_{II}s are represented by great circles that intersect at the C_I direction. The C_I direction is coincident with the pole to the plane that is fitted to the poles to the demagnetization planes (solid triangles). (B) Example of an extreme bias of great circle analysis (Schmidt 1985). Triangles are poles to 10 great circles (not shown) defined by 10 pairs from the two data sets (C_I and C_{II}). Dispersion of the two data sets are equal ($k = 33$). The pole to the plane that is fitted to the poles to demagnetization planes (solid triangles), which is the mean of the great circle intersection points (e.g. Halls 1976), lies mid-way along a great circle between C_I and the inverted C_{II} directions.

near the coastline of Antarctica south of Africa. It is close to the Hervey Group (HG) pole (Li *et al.* 1988), but displaced towards the Comerong Volcanics (CV) pole (Schmidt *et al.* 1986). Indeed the Merrimbula Group overlies the Comerong Volcanics, and the Worange Point Formation is probably slightly older than the Hervey Group. The palaeomagnetic data indicate a low latitude position for

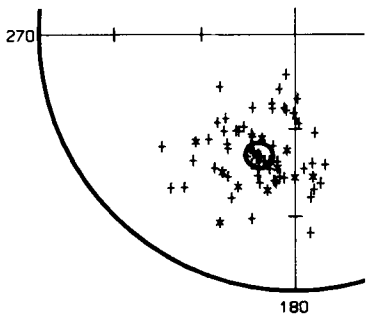

Figure 15. Results of the great circle analysis. '+'s are best estimate directions of the characteristic component on each demagnetization-plane great circle. The best estimate directions were calculated using an iterative technique (McFadden & McElhinny 1988), which incorporates 'sector constraints' (segments of the great circle within which the characteristic component must lie), and 'set-points' (stable endpoint determinations of the characteristic component). The '*'s are the 10 set points. The ellipse is the α_{95} about the mean result. Summary and result of the great circle analysis: 10 setpoints; 62 great circles; 62 sector constraints; two best estimate points fall outside sector constraints; $N = 72$, $R = 69.5199$, $k = 16.13$ Dec. = 196.7, Inc. = 49.3, $\alpha_{95} = 4.3$.

Australia. As discussed, both the Merrimbula Group and the Hervey Group belong to the Late Devonian–Early Carboniferous Lambie Facies. The consistency of the two Lambie poles (HG and WP; Figs 1, 2 and 17) and the pole from the Cannin Basin Limestone (CB; Hurley & Van der Voo 1987) of NW Australia supports the interpretation based on the Lambie Facies overlap assemblage (Figs 1 and 2): the Lachlan Fold Belt was closely tied to interior Australia at least since the Late Devonian (e.g. Brown 1931; Schmidt *et al.* 1986, 1987; Li *et al.* 1988; Powell *et al.* 1990).

The progression and large spread of the pole positions (Fig. 17) derived from (1) the Late Silurian?–Early Devonian Snowy River Volcanics (SRV; Schmidt *et al.* 1987), (2) the Middle–Late Devonian Comerong Volcanics (CV; Schmidt *et al.* 1986), and (3) the Late Devonian–Early Carboniferous Lambie Facies (HG & WP: Li *et al.* 1988; Thrupp, Kent & Schmidt 1988; this study) suggest angular apparent polar wander rates exceeding $1°\,Myr^{-1}$ during the Devonian. However, the age of magnetization of the Worange Point Formation and Hervey Group red beds could be considerably younger than the age of deposition, in which case the implied rates of plate motion are slower.

The magnetization of the Canning Basin Limestone from NW Australia may also be considerably younger than the Late Devonian age of the rocks. This possibility was suggested by Schmidt *et al.* (1987), as an alternative to the displaced Tasman terrane model (Hurley & Van der Voo 1986; Van der Voo 1988), to explain the seemingly excessive difference in the positions of the Canning Basin Limestone (CB) and Comerong Volcanics (CV) poles. The principal

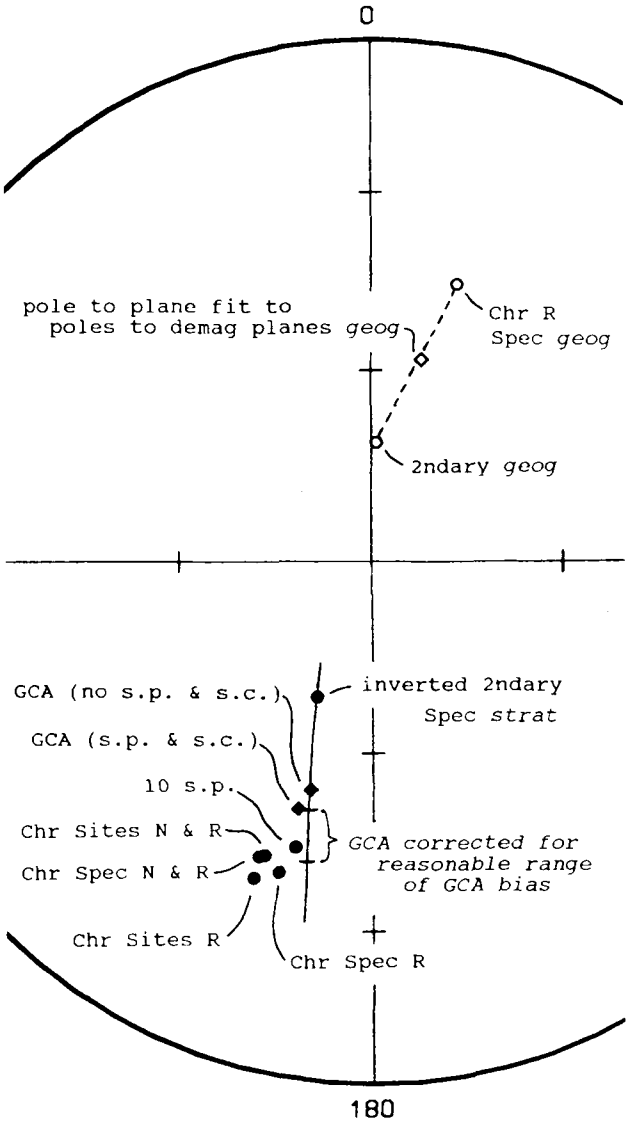

Figure 16. Comparison of mean results calculated in various ways, and illustration of great circle analysis bias. The result of the great circle analysis (GCA) without set points (s.p.) or sector constraints (s.c.) is expected to be biased toward the inverted mean direction of the secondary component along a great circle through the two of them. Also as expected, the great circle intersection estimate of the secondary component (pole to the plane fit to poles to demagnetization planes in geographic coordinates) is biased toward the mean characteristic component (in geographic coordinates). For the great circle analysis in stratigraphic coordinates, the bias (Schmidt 1985) is estimated to be between 4° and 12°; the range of the sought-after characteristic component derived from the corrected GCA result is shown. The result of the GCA analysis including set points and sector constraints is displaced toward the conventional estimates of the characteristic component because of the set points. There is little difference between the results derived from site-mean, all specimens, only reverse polarity, both polarities. The palaeomagnetic pole is derived from specimens with a reverse polarity characteristic component.

arguments for an essentially original age of magnetization of the Canning Basin Limestones are that the rocks have never been heated appreciably, and that several stratigraphically controlled reversals are present (Hurley 1986; Hurley &

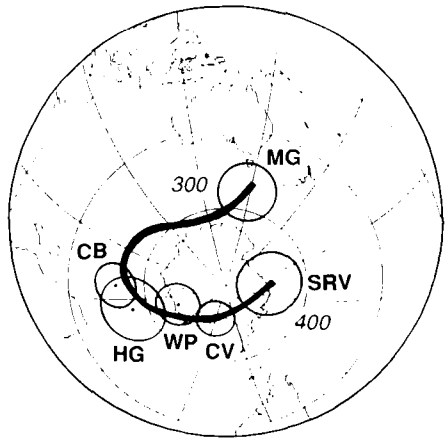

Figure 17. Most reliable Devonian–Carboniferous palaeomagnetic poles from Australia. Pole Mnemonics: SRV; Early Devonian Snowy River Volcanics (Schmidt *et al.* 1987). CV; Middle Late Devonian Comerong Volcanics (Schmidt *et al.* 1986). WP; Late Devonian Worange Point Formation (this study). HG; Late Devonian–Early Carboniferous Hervey Group (Li *et al.* 1988). CB; Late Devonian Canning Basin Limestone (Hurley & Van der Voo 1987). MG; Late Carboniferous Main Glacial Stage (Irving 1966).

Van der Voo 1987). Thus remagnetization by a major thermal or short-lived chemical phenomenon is precluded, but the magnetization may be associated with diagenesis that could be significantly younger than the age of deposition.

Utilizing cross-cutting textural relationships, relative trace element concentrations detected by cathodeluminescence, and carbon and oxygen isotopic data, Hurley (1986) differentiated six distinct diagenetic events that affected the Canning Basin Limestones. There were two episodes of burial: (1) Late Devonian to Early Carboniferous; (2) Late Carboniferous to Permian. Haematite carries a major portion of the remanence in several of the Canning Basin Limestone localities. A constraint on the age of haematite at some sites is provided by a calcite cement that post-dates the haematite, and is post-Late Carboniferous, but pre-Late Permian (Hurley 1986). Thus, the haematite, which is probably the main source of the remanent magnetization at some sites, is constrained only to be pre-Late Permian.

Stromatolites in the Canning Basin limestone section that has multiple reversals are made of filaments of *Frutexites*, which are mat-forming cynobacteria that concentrated metals from sea water. The primary precipitates of *Frutexites* were probably iron hydroxides, which with shallow burial, alter to haematite. Thus, the remanence carried by haematite in the *Frutexites* limestone section is probably associated with diagenesis after shallow burial. Five reversals occur within 15 cm of limestone section. The limestone accumulation rate based on the time span indicated by six conodont zones is 1.8 mm per 1000 yr (Hurley 1986; Hurley & Van der Voo 1986, 1987). Accordingly, the 14.5 cm section would have been deposited in ~81 000 yr, or ~95 000 yr, allowing for volume reduction due to 15 per cent compaction. If the remanence was acquired at a rate similar to the deposition, the implication is that five polarity reversals occurred in less than 100 000 yr, a reversal periodicity of ~40 000 yr. This is unlikely: the minimum periodicity of polarity reversals since the

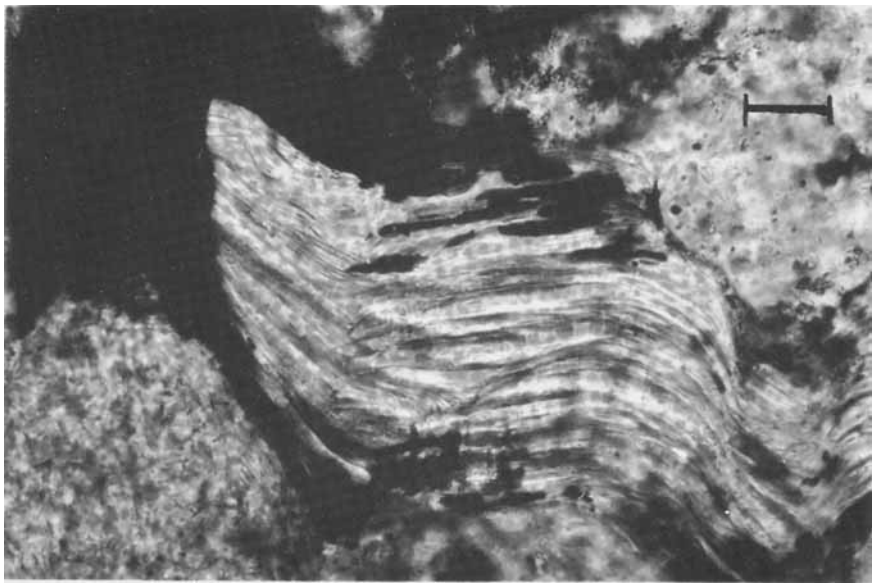

Figure 18. Photomicrograph of a thin section of the Worange Point sandstone showing a buckled detrital grain of chlorite after biotite with authigenic, euhedral crystalline haematite in the mica folia. Width of photo is ~200 μm; bar scale at upper right is ~20 μm. The specimen is from flat-lying sandstone strata (Site 6) with no evidence of cleavage in outcrop. The buckled micas are associated with a ubiquitous, incipient, subvertical cleavage that is folded, but probably formed during the beginning stages of the mid-Carboniferous deformation (Rixon *et al.* 1983). If the authigenic haematite that formed at this stage carries an appreciable portion of the high blocking temperature remanent magnetization, the characteristic component could be a *syn-deformational pre-folding remanence.*

mid-Jurassic, as inferred from the sea-floor anomalies, is ~150 000 yr at ~10 Ma (McFadden & Merrill 1984). Perhaps the acquisition of magnetization accompanied a phase of slightly increased temperatures (~100 °C), during the Late Devonian to Early Carboniferous burial, that Arne *et al.* (1989) suggested for the north Canning Basin region to explain the results of an analysis of apatite fission tracks.

The age of magnetization of the Lambie Facies red beds is also poorly constrained. Although there are arguments for a pre-folding acquisition of magnetization in both the Hervey Group and Worange Point Formation red beds, the possibility of syn-deformational acquisition of magnetization should not be discounted. In thin sections of the Worange Point Formation, buckled detrital mica flakes are evident even in flat-lying, uncleaved sandstones. Typically, the biotite is altered to chlorite with translucent euhedral tabular prisms of haematite (5–30 μm long) along the cleavage folia (Fig. 18). The buckling of the micas is associated with the incipient cleavage that formed during the early stages of deformation, but pre-dates the folding (Rixon *et al.* 1983). Alteration of biotite, and the associated growth of haematite probably occurred during the early stages of deformation. Much more abundant equant, sub-euhedral crystalline haematite (6–60 μm), which is not within any mafic mineral, may be contemporaneous. If enough haematite formed during the early stages of deformation, the rocks could have a *syn-deformational, pre-folding* remanence that would be mid-Carboniferous in age.

Despite the lack of a 'fold test', a pre-folding acquisition of remanence for the uncleaved Hervey Group red beds is advocated by Li *et al.* (1988). The anisotropy of magnetic susceptibility (AMS) defines a planar fabric in the Hervey Group red beds that roughly parallels bedding in the non-cleaved rocks, but is nearly parallel to the cleavage in one site with well-developed cleavage. Li *et al.* (1988) suggest that the bedding-parallel AMS fabric is due to pre-deformational compaction of haematite produced during the early stages of diagenesis. They argue that because the cleaved rock with AMS fabric close to cleavage has discordant remanence, the uncleaved rock with bedding-parallel AMS fabric has a pre-deformational remanence. It should be emphasized, however, that the grains defining the AMS fabric need not be the same as those carrying the remanence (e.g. Herrero-Bervera & Urrutia-Fucuganchi 1988; McCabe & Elmore 1989). A bedding parallel AMS fabric reflecting a depositional or compaction fabric can be preserved regardless of the source and habit of the haematite that carries the remanence. The difference between the AMS fabric and remanence in the uncleaved and markedly cleaved Hervey Group rocks could be a consequence of volume reduction resulting in concentration and alignment of magnetic grains within cleavage seams. Preservation of a bedding-parallel AMS fabric, however, is not conclusive evidence for a pre-deformational remanence in the uncleaved rocks.

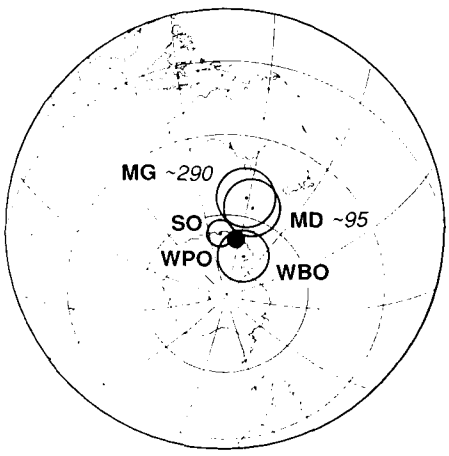

Figure 19. *Overprint* Poles from Late Silurian–Early Carboniferous rocks compared to reliable reference poles with similar positions. Pole Mnemonics: SO; combined BO and SRO overprint poles (post-mid-carboniferous) in Buchan Caves Limestones and secondary component in Snowy River Volcanics; (Schmidt *et al.* 1987). WPO; overprint (post-mid-carboniferous, Late Cretaceous?) in the Worange Point Fm (this study). WBO; overprint (post-mid-Carboniferous, Late Cretaceous?) in Early Devonian Waratah Bay limestones (G. A. Thrupp, preliminary unpublished data). MG; main glacial stage, Late Carboniferous pole (Irving 1966). MD; Mount Dromedary, mid-Cretaceous pole (Schmidt 1976).

The high unblocking-temperature normal component in many of the Worange Point samples is a composite direction comprising a steep post-folding CRM and an early more shallow direction. The means of the reverse and normal polarity subsets from both the Hervey Group and Worange Point Formation data are more nearly antipodal after correction for tilt. For the Worange Point data, this is consistent with the suggestion that isolation of a univectorial normal characteristic component has not been achieved: the steep residual CRM component disperses with correction for tilt. The Worange Point polarity subset means are ~10° from being antipodal; they are distinct at ~50 per cent confidence. The Hervey Group subsets are ~20° from being antipodal; distinct at 78 per cent confidence.

Failure of both data sets to pass a 'reversal test' at high confidence implies that either secondary components are incompletely removed or the subset means do not average secular variation adequately. The absence of low-coercivity magnetic mineral in the Worange Point specimens subjected to IRM acquisition experiments, indicates that any pre-existing detrital magnetite, titanomagnetite, or maghaemite, has been completely oxidized to haematite. Such complete intrastratal haematization probably takes millions of years (Walker *et al.* 1981). Thus, there is no doubt that acquistion of magnetization in these red beds took place over a period long enough to average enough secular variation. One could appeal to significant long-term departure from an axial geocentric dipole magnetic field, but at least for the Tertiary, asymmetry of the non-dipole components for normal and reverse fields is far too small to cause significant departure from an antipodality (e.g. chapter 6 of Merrill & McElhinny 1983). As discussed, the high-temperature normal directions in the Worange Point rocks probably comprise a post-folding, steep, normal component, and a pre-folding, shallower component; in many cases, the two CRMs are inseparable because the unblocking temperature spectra completely overlap. The HG result, like the WP result, is probably contaminated by a residual overprint.

The fact that a stable, well-defined characteristic component is present in less than half of the Worange Point Formation and Hervey Group samples attests to the complexity and variability of the nature of the remanent magnetization in these red beds. The age of magnetization is uncertain, and its nature is poorly understood. Nonetheless, the close agreement between the Hervey Group and Worange Point Formation pole positions lends credence to the position of the poles.

WHAT IS THE AGE OF THE POST-FOLDING OVERPRINT?

The pole position indicated by the post-folding magnetization in the Worange Point Formation is close both to the Late Carboniferous and early Late Cretaceous Australian reference poles (Fig. 19). The mean overprint direction differs by ~7° from the present field direction, and by ~15° from the axial geocentric dipole field direction at the Merimbula region. Contamination of a Late Carboniferous or Late Cretaceous overprint by a component of remanence recording either the present field or a recent dipole field, would shallow the overprint, resulting in an overprint pole farther from the locality than the overprint reference pole (a 'far-sided' south pole). The positions of palaeomagnetic poles indicated by post-mid Carboniferous overprints in the Worange Point Formation, the Snowy River Volcanics and overlying Buchan Caves Limestones (Schmidt *et al.* 1987), and the Waratah Bay Limestones (G. A. Thrupp, unpublished data) are all nearly identical (Fig. 19). Because the overprint directions are all of normal polarity, and because the Australia/Antarctica rifting and the opening of the Tasman Sea began during the mid-Cretaceous normal superchron, a mid-Cretaceous age for the overprint seems likely. Reset fission-track ages from apatites in Palaeozoic granitic bodies in SE Australia show a rapid decrease in age toward the east, reflecting increasing temperature with proximity to the Tasman Sea coastline (Fig. 20; Moore, Gleadow & Lovering 1986). The 80–100 Myr fission-track ages, which are completely reset, record cooling, which followed rifting that led to opening of the Tasman Sea. The mid-Cretaceous thermal disturbance of the Tasman coastline is also recorded by remagnetization in the Sydney Basin (Schmidt & Embleton 1981).

For several reasons Schmidt *et al.* (1987) favoured a Late Carboniferous age for the secondary magnetization in the Snowy River Volcanics and the overprint in the overlying Buchan Caves limestones: (1) The overprint pole positions are distinct (at 95 per cent confidence) from the Late Cretaceous reference pole positions. (2) They fall on the

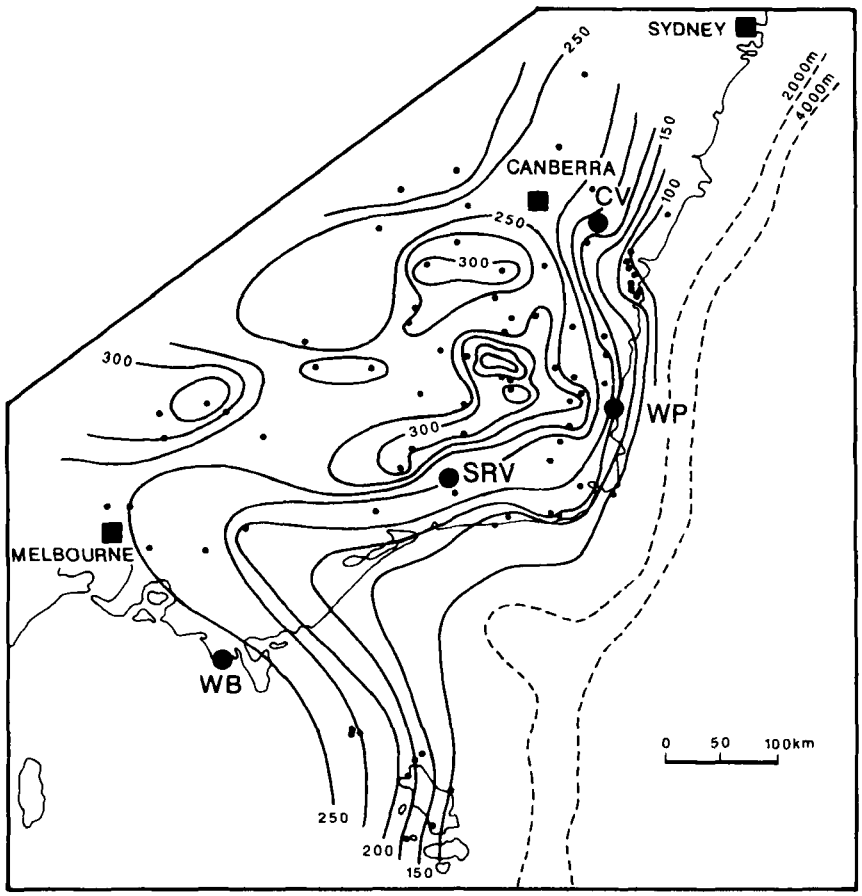

Figure 20. Map of a portion of SE Australia with contours showing fission-track ages from apatite crystals from mid–late Palaeozoic plutonic rocks (Moore *et al.* 1986). Inland, resetting is less severe than near to the coast. The thermal event is believed to be the Early Cretaceous rifting, the beginning of the opening of the Tasman Sea; the magnetic overprinting is probably related. The locations of four palaeomagnetic studies are shown: CV—Comerong Volcanics (Schmidt *et al.* 1986); SRV—Snowy River Volcanics and Buchan Caves Limestone (Schmidt *et al.* 1987); WP—Worange Point Formation (this study); WB—Waratah Bay Limestones (G. A. Thrupp, preliminary unpublished data).

path between the Early and Late Carboniferous reference poles. (3) They are nearly identical to the Late Carboniferous Patterson Toscanite pole (Irving 1966). (4) The apatite fission-track ages are less reset in the Snowy River vicinity than along the coast, which indicates that the Late Cretaceous heating was quite minor in the Snowy River vicinity.

Although remagnetization at the end of the phase of mid-Carboniferous deformation that produced the folding is reasonable, the possibility that the Snowy River overprint is Late Cretaceous should not be ruled out. Each of the above arguments for a Late Carboniferous age can be countered: (1) Contamination of a Late Cretaceous overprint direction by a recent dipole overprint could be responsible for the difference between the positions of the overprint poles and the Late Cretaceous reference poles. (2) The Carboniferous Australian APWP is poorly defined and controversial; recent versions (Li, Powell & Schmidt 1989; Li *et al.* 1990b; Schmidt *et al.* 1990) would be simpler if the Snowy River overprint poles were omitted. (3) The Patterson Toscanite pole (Irving 1966) is derived from only one lava flow, and therefore does not average enough secular variation to be a valid palaeomagnetic pole; it is a VGP that need not lie on the APWP. (4) The reset fission-track data do not explain the distribution of the magnetic overprints. For example, the fission-track data suggest that the Comerong Volcanics should have been affected more strongly than the rocks at the Snowy River and Waratah Bay localities, but the Comerong Volcanics do not have a well-defined consistent secondary component. The fission-track data set, however, is rather sparse, and discordant zones may be associated with faulting (D. Arne, personal communication, 1988).

The steep normal secondary component in the Worange Point Formation, which resides in haematite, is unblocked typically between 200° and 500 °C. In many specimens, however, it persists to higher temperatures. The partial resetting of the apatite fission-track dates in the vicinity of the Worange Point Formation suggests temperatures of about 100 °C before cooling at ~80 Ma (Moore *et al.* 1986; D. Arne, personal communication, 1989). Thermal activation curves for haematite (Pullaiah *et al.* 1975), which are corroborated by experimental data (Kent & Miller 1987) and further theoretical considerations (Enkin & Dunlop 1988), predict that a viscous partial thermal remanent magnetization (VPTRM) produced by a temperature of ~100° maintained for a couple of million years would be unblocked by heating to ~400 °C for about 30 min. Thus it is feasible that much of the steep normal secondary component is a VPTRM attributable to elevated temperatures associated with the Tasman rifting during the mid-Cretaceous. However, the higher unblocking temperature overprint is probably CRM that is roughly contemporaneous with the VPTRM. Oxidation of remaining ferrous iron, to new haematite would have been accelerated during elevated temperatures associated with Tasman rifting.

The temperatures indicated by the fisson-track data seem too low to have caused major resetting of the magnetization inland of the Tasman Sea, but secondary viscous remanent magnetization (VRM) can have unblocking temperatures that exceed those predicted by single-domain theory (Enkin & Dunlop 1988; Jackson & Van der Voo 1986). As is suggested above for the Worange Point Formation, chemical alterations resulting in the growth of new magnetic phases probably play a role (e.g. McCabe & Elmore 1989). Variability in permeability of different lighologies may affect the degree of overprinting. In regions away from the coastline, the steep overprint may be related to the mid-Carboniferous Kanimblan Orogeny, whereas close to the coastline it may be a consequence of the Cretaceous rifting.

CONCLUSIONS

A well-defined steep secondary component of magnetization, which is manifested both as VPTRM and CRM, post-dates the mid-Carboniferous folding of the Worange Point Formation (Fig. 8). The overprint pole (Fig. 19) is nearly identical to overprint poles derived from Late Permian to Jurassic rocks of the Sydney Basin (Schmidt & Embleton 1981), Late Devonian limestones of Waratah Bay (G. A. Thrupp, unpublished data), and Early and Late Devonian volcanics and limestones of the Snowy River region (Schmidt *et al.* 1987). The exclusively normal polarity of the overprints is consistent with acquisition during the mid-Cretaceous normal polarity super-chron. Probably the overprinting is related to the Australia/Antarctica rifting and the opening of the Tasman Sea, which began during the mid-Cretaceous normal superchron. Partially reset fission-track ages from Palaeozoic plutonic rocks decrease rapidly with proximity to the rifted coastal margin (Fig. 20; Moore *et al.* 1986).

The palaeomagnetic pole (Fig. 17) indicated by characteristic magnetization preserved in the Worange Point Formation is close to the Hervey Group pole (Li *et al.* 1988; HG on Fig. 17). Both results are derived from red beds of the Late Devonian–earliest Carboniferous Lambie Facies in the Lachlan Fold Belt. The consistency of these two pole positions and the Canning Basin Limestone pole (CB; Hurley & Van der Voo 1986) supports the concept that the Lambie Facies sediments overlap the tectonic elements of the southeast Tasman Fold Belt (Fig. 1) precluding major displacement of any Tasman terranes since the Late Devonian. The overlap assemblage provides an earlier constraint than the palaeomagnetic data because for CB, HG, and WP (this study) the acquisition of magnetization is suggested to post-date the deposition.

The only reliable result from the Lachlan Fold Belt that is derived from rocks old enough to be potentially exotic with respect to the Australian craton is the palaeomagnetic pole obtained by Schmidt *et al.* (1987) from the late Silurian or early Devonian Snowy River Volcanics (SRV). Nonetheless, the position of the SRV pole seems compatible with the SE Lachlan Fold Belt being essentially fixed, with respect to the Australian craton, since the latest Silurian. The same is indicated by a tectonostratigraphic analysis of the Lachlan Fold Belt (Leitch & Scheibner 1987).

The Late Devonian and younger palaeomagnetic poles derived from rocks of the Lachlan Fold Belt are applicable to Australia and Gondwana as a whole. The mid-Devonian through early Carboniferous segment of the Gondwanan APWP is well defined. However, the paucity of reliable palaeomagnetic data from Gondwana during the Silurian and the Carboniferous, both of which were periods of rapid

Gondwanan drift, allows great leeway in extending the Devonian pole path back to the Ordovician or forward to the Permian.

ACKNOWLEDGMENTS

A Macquarie University Research Fellowship supported G.T. Grants from ARC (A38831488) and the CSIRO/Macquarie University collaborative research scheme funded the research. Funds from the Geological Society of Australia enabled D.K. to attend a conference and participate in the field work. We thank C. Klootwijk, J. Giddings, and W. Sunata for their collaboration and assistance in the field, and D. Arne for generous informative correspondence and for sharing unpublished fission-track data.

REFERENCES

Arne, D. C., Green, P. F., Duddy, I. R., Gleadow, A. J. W., Lambert, I. B. & Lovering, J. F., 1989. Regional thermal history of the Lennard Shelf, Canning Basin, from apatite fission track analysis: Implications for formation of Pb–Zn ore deposits, *Aust. J. Earth Sci*, **36**, 495–513.

Baag, C. B. & Helsley, C. E., 1974. Shape analysis of paleosecular variation data, *J. geophys. Res.*, **79**, 4923–4932.

Benson, W. N., 1922. Materials for study of the Devonian Paleontology of Australia, *Rec. geol. Surv. N. S. W.*, **10**, 83–204.

Brown, I. A., 1931. The stratigraphic and structural geology of the Devonian rocks of the south coast of New South Wales, *Proc. Linn. Soc. N. S. W.*, **16**, 461–496.

Conolly, J. R. II, 1969. Upper Devonian Series of the southern and coastal Highlands Fold Belt, in The geology of New South Wales, *J. geol. Soc. Aust.*, **16**, part 1.

Cox, A., 1970. Latitude dependence of the angular dispersion of the geomagnetic field, *Geophys. J. R. astr. Soc.*, **20**, 253–269.

Cox, A. & Gordon, R. G., 1984. Paleolatitudes determined from paleomagnetic data from vertical cores, *Rev. Geophys. Space Phys.*, **22**, 47–72.

Dekkers, M. J. & Linssen, J. H., 1989. Rockmagnetic properties of fine-grained natural low-temperature haematite with reference to remanence acquisition mechanisms in red beds, *Geophys. J. Int.*, **99**, 1–18.

Dunlop, D. J., 1972. Magnetic mineralogy of unheated and heated red sediments by coercivity spectrum analysis, *Geophys. J. R. astr. Soc.*, **27**, 37–55.

Embleton, B. J. J., 1972. The palaeomagnetism of some Palaeozoic sediments from Central Australia, *J. Proc. R. Soc. N. S. W.*, **105**, 86–93.

Embleton, B. J. J., McElhinny, M. W., Crawford, A. R. & Luck, G. R., 1974. Palaeomagnetism and the tectonic evolution of the Tasman orogenic zone, *J. geol. Soc. Aust.*, **21**, 187–193.

Enkin, R. J. & Dunlop, D. J., 1988. The demagnetization temperature necessary to remove viscous remanent magnetization, *Geophys. Res. Lett.*, **15**, 514–517.

Fergusson, C. L., Cass, R. A. F., Collins, W. S., Craig, G. Y., Crook. K. A. W., Powell, C.McA, Scott, P. A. & Young, G. C., 1979. The Upper Devonian Boyd Volcanic Complex, Eden, New South Wales, *J. geol. Soc. Aust.*, **26**, 87–105.

Fisher, Sir R., 1953. Dispersion on a sphere, *Proc. R. Soc. Lond.*, **217**, 295–305.

Goleby, B. R., 1980. Early Palaeozoic palaeomagnetism in south east Australia, *J. Geomagn. Geoelect.*, **32**, Suppl. III, SIII 11–SIII 21.

Halls, H. C., 1976. A least-squares method to find a remanence direction from converging remagnetization circles, *Geophys. J. R. astr. Soc.*, **45**, 297–304.

Harrison, C. G. A., 1980. Secular variation and excursions of the earth's magnetic field, *J. geophys. Res.*, **85**, 3511–3522.

Herrero-Bervera, E & Urrutia-Fucuganchi, J., 1988. A magnetic study of some remagnetized Upper Jurassic red beds, *EOS, Trans. Am. geophys. Un.*, **69**, 1170.

Hurley, N. F., 1986. Geology of the Oscar Range Devonian reef complex, Canning Basin, Western Australia, *PhD thesis*, University of Michigan.

Hurley, N. F. & Van der Voo, R., 1986. Late Devonian magnetostratigraphy from a condensed limestone, Canning Basin, Western Australia (abstract), *EOS, Trans. Am. geophys. Un.*, **67**, 265.

Hurley, N. F. & Van der Voo, R., 1987. Paleomagnetism of Upper Devonian reefal limestones, Canning Basin, Western Australia, *Bull. geol. Soc. Am.*, **98**, 138–146.

Idnurm, X. Y. & Schmidt, P. W., 1986. Laterisation Processes, *Geol. Surv. India Mem.*, **120**, 79–88.

Irving, E., 1966. Paleomagnetism of some Carboniferous rocks from New South Wales and its relation to geological events, *J. geophys. Res.*, **71**, 6025–6051.

Jackson, M. & Van der Voo, R., 1986. Thermally activated viscous remanence in some magnetite- and hematite-bearing dolomites, *Geophys. Res Lett.*, **13**, 1434–1437.

Kirschvink, J. L., 1980. The least-square line and plane and the analysis of palaeomagnetic data, *Geophys. J. R. astr. Soc.*, **62**, 699–718.

Kent, D. V. & Miller, J. D., 1987. Redbeds and thermoviscous magnetization theory, *Geophys. Res. Lett.*, **14**, 327–330.

Leitch, E. C. & Scheibner, E., 1987. Stratotectonic terranes of the eastern Australian Tasmanides, in *Terrane Accretion and Orogenic Belts*, eds Leitch, E. C. & Scheibner, E., Am. geophys. Union, Washington, DC.

Li, Z. X., Schmidt, P. W. & Embleton, B. J. J., 1988. Paleomagnetism of the Hervey Group, central New South Wales and its tectonic implications, *Tectonics*, **7**, 351–367.

Li, Z. X., Powell, C.McA. & Schmidt, P. W., 1989. Syn-deformational remanent magnetization of the Mount Eclipse Sandstone, central Australia, *Geophys. J. Int.*, **99**, 205–222.

Li, Z. X., Powell, C. McA., Embleton, B. J. J. & Schmidt, P. W., 1990a. New palaeomagnetic results from the Amadeus Basin and their implications for stratigraphy and tectonics, in *Geological and Geophysical Studies of the Amadeus Basin, Central Australia*, ed. Korsch, R. J., BMR Bull., in press.

Li, Z. X., Powell, C. McA, Thrupp, G. A. & Schmidt, P. W., 1990b. Australian Palaeozoic Palaeomagnetism and Tectonics—II: A revised apparent polar wander and palaeogeography, *J. struct. Geol.*, **12**, 567–575.

Luck, G. R., 1973. Palaeomagnetic results from Palaeozoic rocks of southeast Australia, *Geophys. J. R. astr. Soc.*, **32**, 35–52.

Merrill, R. T. & McElhinny, M. W., 1983. *The Earth's Magnetic Field*, Academic Press, London.

McCabe, C. & Elmore, R. D., 1989. The occurrence and origin of Late Paleozoic remagnetization in the sedimentary rocks of North America, *Rev. Geophys.*, **27**, 471–494.

McElhinny, M. W., 1973. *Palaeomagnetism and Plate Tectonics*, Cambridge University Press, Cambridge, UK.

McElhinny, M. W. & Embleton, B. J. J., 1974. Australian palaeomagnetism and the Phanerozoic plate tectonics of eastern Gondwanaland, *Tectonophysics*, **22**, 1–29.

McFadden, P. L. & Jones, D. L., 1981. The fold test in palaeomagnetism, *Geophys. J. R. astr. Soc.*, **67**, 53–58.

McFadden, P. L. & Lowes, F. J., 1981. The discrimination of mean directions drawn from a Fisher distribution, *Geophys. J. R. astr. Soc.*, **67**, 19–33.

McFadden, P. L. & Merrill, R. T., 1984. Lower mantle convection and geomagnetism, *J. geophys. Res.*, **89,** 3354–3362.

McFadden, P. L. & McElhinny, M. W., 1988. The combined analysis of remagnetization circles and direct observations in palaeomagnetism, *Earth planet. Sci. Lett.*, **87,** 161–172.

McIlveen, G. R., 1975. The Eden–Comerong–Yalwal rift zone and the contained gold mineralization, *Rec. geol. Surv. N. S. W.*, **16,** 245–277.

Moore, M. E., Gleadow, A. J. W. & Lovering, J. F., 1986. Thermal evolution of rifted continental margins: new evidence from fission tracks in basement apetites from south-eastern Australia, *Earth planet. Sci. Lett.*, **78,** 255–270.

Morel, P. & Irving, E., 1978. Tentative palaeocontinent maps for the Early Phanerozoic and Proterozoic, *J. Geol.*, **86,** 535–561.

Powell, C. McA., 1983. Geology of N. S. W. South Coast, *SGTSG Field Guide 1,* Geol. Soc. Aust., Sydney.

Powell, C. McA., 1984. Ordovician to Carboniferous, in *Phanerozoic Earth History of Australia,* pp. 290–340, ed. Veevers, J. J., Clarendon Press, Oxford.

Powell, C. McA., Li, Z. X., Thrupp, G. A. & Schmidt, P. W., 1990. Australian Palaeozoic Palaeomagnetism and Tectonics—I: Tectonostratigraphic terrane constraints from the Tasman Fold Belt, *J. struct. Geol.*, **12,** 553–565.

Pullaiah, G., Irving, E., Buchan, K. L. & Dunlop, D. J., 1975. Magnetization changes caused by burial and uplift, *Earth planet. Sci. Lett.*, **28,** 133–143.

Rixon, L. K., Bucknell, W. R. & Rickard, M. J., 1983. Mega kink folds and related structures in the Upper Devonian Merrimbula Group, south coast of New South Wales, *J. geol. Soc. Aust.*, **30,** 277–293.

Scheibner, E., 1985. Suspect terranes in the Tasman Fold Belt System, Eastern Australia, in *Tectonostratigraphic Terranes in the Circum-Pacific Region,* Earth Science Series, Number 1, pp. 493–514, ed. Howell, D. G., Circum-Pacific Council for Energy and Mineral Resources, Houston.

Schmidt, P. W., 1976. The Late Palaeozoic and Mesozoic Palaeomagnetism of Australia, *PhD thesis,* Australian National University.

Schmidt, P. W., 1985. Bias in converging great circle methods, *Earth planet. Sci. Lett.*, **72,** 427–432.

Schmidt, P. W. & Embleton, B. J. J., 1981. Magnetic overprinting in southeastern Australia and the thermal history of its rifted margin, *J. geophys. Res.*, **86,** 3998–4008.

Schmidt, P. W. & Embleton, B. J. J., 1987. A critique of palaeomagnetic results from Australian Palaeozoic fold belts and displaced terranes, in *Terrane Accretion and Orogenic Belts,* Geodynamic Series, Vol. 19, pp. 21–23, eds Leitch, E. C. & Scheibner, E., American Geophysical Union, Washington, DC.

Schmidt, P. W. & Morris, W. A., 1977. An alternative view of the Gondwana Paleozoic apparent polar wander path, *Can. J. Earth Sci.*, **14,** 2674–2678.

Schmidt, P. W., Embleton, B. J. J. & Palmer, H. C., 1987. Pre- and post-folding magnetizations from the early Devonian Snowy River Volcanics and Buchan Caves Limestone, Victoria, *Geophys. J. R. astr. Soc.*, **91,** 155–170.

Schmidt, P. W., Embleton, B. J. J., Cudahy, T. J. & Powell, C. McA., 1986. Prefolding and premegakinking magnetizations from the Devonian Comerong volcanics, New South Wales, Australia, and their bearing on the Gondwana pole path, *Tectonics,* **5,** 135–150.

Schmidt, P. W., Powell, C. McA., Li, Z. X., & Thrupp, G. A., 1990. Reliability of Palaeozoic palaeomagnetic poles and APWP of Gondwanaland, *Tectonophysics,* in press.

Steiner, J., 1975. The Merrimbula Group of the Eden-Merrimbula Area, N. S. W., *J. Proc. R. Soc. N. S. W.*, **108,** 37–51.

Taylor, G. & Mayer, W., 1990. Depositional environments and palaeogeography of the Worange Point Formation, New South Wales, *Aust. J. Earth Sci.*, **37,** 227–239.

Thrupp, G. A., Kent, D. V. & Schmi, P. W., 1988. Preliminary palaeomagnetic results from Late Devonian redbeds of southeast Australia (abstract), *EOS, Trans. Am. geophys. Un.*, **69,** 1170.

VandenBerg, A. H. M., 1976. Silurian–Middle Devonian, Eastern Victoria, in *Geology of Victoria,* Special Publ. Geol. Soc. Aust., no. 5, eds Douglas, J. G. & Ferguson, J. A., Melbourne.

Van der Voo, R., 1988. Paleozoic paleogeography of North America, Gondwana, and intervening displaced terranes: comparisons of paleomagnetism with paleoclimatology and biogeographical patterns, *Bull. geol. Soc. Am.*, **100,** 311–324.

Walker, T. R., Larson, E. E. & Hoblitt, R. P., 1981. Nature and origin of hematite in the Moenkopi Formation (Triassic), Colorado Plateau: a contribution to the origin of magnetism in red beds, *J. geophys. Res.*, **86,** 317–333.